



TITLE:

Pd(II)-promoted direct cross-coupling reaction of arenes via highly regioselective aromatic C-H activation: a theoretical study.

AUTHOR(S):

Ishikawa, Atsushi; Nakao, Yoshihide; Sato, Hirofumi; Sakaki, Shigeyoshi

CITATION:

Ishikawa, Atsushi ...[et al]. Pd(II)-promoted direct cross-coupling reaction of arenes via highly regioselective aromatic C-H activation: a theoretical study.. Dalton transactions (Cambridge, England : 2003) 2010, 39(13): 3279-3289

ISSUE DATE:

2010-04-07

URL:

<http://hdl.handle.net/2433/139432>

RIGHT:

© The Royal Society of Chemistry 2010; この論文は出版社版ではありません。引用の際には出版社版をご確認ご利用ください。 ; This is not the published version. Please cite only the published version.

Pd(II)-Catalyzed Direct Cross-Coupling Reaction of Arenes via Highly Regioselective Aromatic C-H Activation: A Theoretical Study[†]

Atsushi Ishikawa,^a Yoshihide Nakao,^a Hirofumi Sato,^a and Shigeyoshi Sakaki^{*a,b}

^a*Department of Molecular Engineering, Graduate School of Engineering, Kyoto University,
Nishikyo-ku, Kyoto 615-8510, Japan, and* ^b*Fukui Institute for Fundamental Chemistry, Kyoto
University, Nishi-hiraki cho, Takano, Sakyo-ku, Kyoto 606-8301, Japan*

(E-mail: sakaki@moleng.kyoto-u.ac.jp)

† Electronic supplementary information (ESI) available: Complete reference 70, Large and small models for ONIOM method, Potential and Gibbs energy changes in gas phase, Potential and Gibbs energy changes of the C-H activation of benzene and the RE of Ph-Bzq, evaluated with DFT, MP2, MP4(SDQ) and ONIOM(CCSD(T):MP2) methods, Relative potential energies of the first C-H activation, BQ coordination, and the second C-H activation reactions calculated by Hartree-Fock, MP2, MP3, MP4(DQ), MP4(SDQ), and DFT(B3PW91) methods.

Abstract

The direct cross-coupling reaction of arenes catalyzed by $\text{Pd}(\text{OAc})_2$ is synthetically very useful because we do not need haloarene as substrate. This reaction occurs only in the presence of benzoquinone (BQ), interestingly. Our DFT, MP2 to MP4(SDQ), and CCSD(T) computational study elucidated the whole mechanism of this cross-coupling reaction and the key roles of BQ. The first step is heterolytic C-H activation of benzo[*h*]quinoline (HBzq) by $\text{Pd}(\text{OAc})_2$ to afford $\text{Pd}(\text{Bzq})(\text{OAc})$. In $\text{Pd}(\text{Bzq})(\text{OAc})$, the Pd center becomes more electron-rich than in $\text{Pd}(\text{OAc})_2$. Hence, BQ easily coordinates to $\text{Pd}(\text{Bzq})(\text{OAc})$ with low activation barrier to afford a distorted square planar complex $\text{Pd}(\text{Bzq})(\text{OAc})(\text{BQ})$ which is as stable as $\text{Pd}(\text{Bzq})(\text{OAc})$. The second C-H activation of benzene occurs after the BQ coordination with moderate activation barrier and small endothermicity. The final step is the reductive elimination which occurs nearly barrierless. The rate-determining step of the overall reaction is the second C-H activation whose activation barrier is considerably higher than that of the first C-H activation. BQ plays key roles in this reaction, as follows: (i) The phenyl group takes favorable position for the reductive elimination in the presence of BQ, because BQ suppresses the phenyl group to take a position distant from the Bzq in the intermediate $\text{Pd}(\text{Ph})(\text{Bzq})(\text{OAc})(\text{BQ})$. And, (ii) BQ stabilizes the transition state and the product complex of the reductive elimination by the back-donation interaction. In the absence of BQ, the reductive elimination step needs much higher activation barrier. Though it was expected that the BQ coordination accelerates the second C-H activation of benzene by decreasing the electron density of Pd in $\text{Pd}(\text{Bzq})(\text{OAc})$, the activation barrier of this second C-H activation is little influenced by BQ.

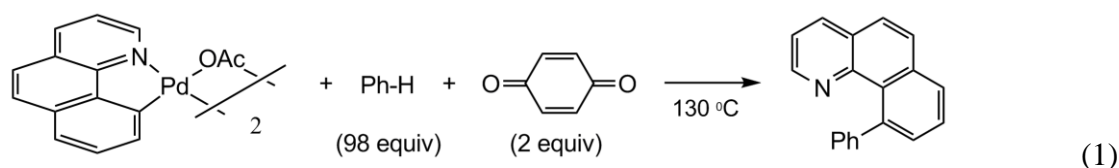
Introduction

In organometallic chemistry, the C-C bond formation reaction catalyzed by transition metal complex is one of the most important research subjects.¹⁻¹² The metal-catalyzed cross-coupling reaction is widely employed for the C-C bond formation such as the Stille coupling reaction¹³ and the Suzuki-Miyaura coupling reaction.¹⁴ High selectivity,¹⁵ functional group tolerance, and use of the mild reaction conditions make these processes sensible choice for the C-C bond formation even in the complicated synthesis of natural product.¹⁶

However, we need organic bromide or organic iodide as the coupling partner in many metal-catalyzed cross-coupling reactions. This requires the preparation step of such organic halides from hydrocarbons. Moreover, the use of the organic halide often leads to the formation of side products that are toxic and also difficult to remove. These are undesirable from both points of view of efficiency and environmentally-friendly reaction. Thus, the direct cross-coupling with non-halogenated substrate is highly desirable, as reported in recent pioneering works.¹⁷⁻²⁰ However, such cross-coupling reaction needs the C-H σ -bond activation which is difficult process unlike the C-X (X = Br or I) bond activation because the C-H σ -bond is much stronger than the C-X bond.

It is expected that the above-mentioned difficulty in the direct cross-coupling reaction can be overcome by using appropriate transition metal catalyst and reaction conditions. Actually, recent experimental works reported that Pd(II) complexes catalyze various homo-coupling of arenes under mild conditions.²¹⁻²³ However, reports on cross-coupling (hetero-coupling) of arenes have been rather limited,²⁴⁻²⁷ though such cross-coupling is synthetically very useful. Another key point of the direct cross-coupling reaction is regioselectivity, because the *ortho*-, *meta*-, and *para*-substituted arenes are often formed as side-product which is difficult to separate. The key point for the high regioselectivity is to activate regioselectively the C-H bond of arene which is also difficult process. For this purpose, the widely used strategy is to employ the ligand-directed C-H activation.²⁸ This is achieved by the coordination of heteroatom such as nitrogen or oxygen to the metal center. Several theoretical studies of the detailed mechanism have been reported.²⁹

Recently, Sanford *et. al.* reported the novel cross-coupling reaction of arenes catalyzed by Pd(II) salt (eq 1).³⁰

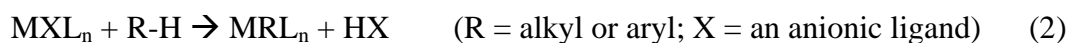


In this reaction, two separate C-H activations occur with high regioselectivity. Their studies focused on stoichiometric cross-coupling reaction between cyclopalladated benzo[h]quinoline (Bzq) complex and benzene at 130 °C, where benzene was used as solvent. The cross-coupling product is 10-phenylbenzo[h]quinoline. Interestingly, this compound is produced only when 2 equivalents of benzoquinone (BQ) are added to the reaction system. These results indicate that BQ plays important roles in the arene cross-coupling reaction. Sanford and coworkers proposed that BQ binds with an initially formed palladium intermediate and promotes the C-H activation of arenes.^{31, 32} This proposal is further supported by experimental results that the use of the methyl-substituted BQ dramatically suppresses the cross-coupling at the *ortho*-position of anisole but increases the cross-coupling at the *meta*- and *para*-positions. These results suggest that BQ coordinates to the Pd center during the arene C-H activation to play important roles not only for reactivity but also for regioselectivity.³⁰

It is of considerable importance to clarify the roles of BQ because such knowledge provides the idea how to achieve the regiocontrol of C-H activation through steric and electronic modifications of an ancillary ligand. To reach the goal of regioselective cross-coupling reaction of arenes, the correct knowledge on the reaction mechanism is also indispensable. However, there are many unclear issues on the reaction mechanism of this arene cross-coupling reaction. For example, though the coordination of BQ with the Pd center is suggested, neither experimental nor theoretical evidence has been presented. Also, it is still unclear how and why the coordination of BQ leads to highly regioselective C-H activation of arene.

Because of the importance of the C-H activation reaction, many theoretical works on this reaction have been carried out.³³⁻⁵³ For instance, Sakaki *et. al.*⁵² successfully disclosed that the C-H

activation of benzene by $\text{Pd}(\text{O}_2\text{CH})_2$ occurs through “heterolytic type C-H activation” (eq 2) unlike “C-H activation by oxidative addition” (eq 3).⁵²



This type of C-H activation mechanism is also studied experimentally and understood as “proton abstraction mechanism”.^{54, 55}

In this paper, we wish to report the theoretical investigation of the arene cross-coupling reaction between HBzq and benzene catalyzed by $\text{Pd}(\text{OAc})_2$. Our purposes here are (i) to clarify the characteristics of the transition states and the important intermediates such as the $\text{Pd}(\text{II})$ -BQ complex, (ii) to present the potential energy profile of the entire catalytic process, and (iii) to elucidate the key roles of BQ, i.e. how and why this cross-coupling reaction regioselectively occurs in the presence of BQ but does not in the absence of BQ.

Computational Details

Geometry optimization was carried out with the DFT method using B3PW91 functional.⁵⁶⁻⁵⁸

Frequency analysis was made with the same method. Möller-Plesset perturbation theory (MP2 to MP4(SDQ)) was used for evaluation of energy changes. Energy changes were also evaluated with the ONIOM method in which the CCSD(T) method was employed for the higher level calculation of the important moiety and the MP2 method was employed for the lower level calculation.

Two basis set systems (BS-I and BS-II) were employed for calculations; In BS-I, Los Alamos effective core potentials (ECPs) were used to replace core electrons of Pd and (341/321/31) basis set was used to represent its valence electrons.⁵⁹ Usual 6-31G(d) basis sets⁶⁰ were used for carbon, nitrogen, oxygen, and hydrogen atoms. In BS-II, Stuttgart-Dresden-Bonn ECPs were used to replace the core electrons of Pd and (8881/7771/661/1) basis set was used for the valence electrons.⁶¹ Dunning cc-pVDZ basis sets⁶² were used for carbon, nitrogen, oxygen, and hydrogen atoms. The

BS-I was used for geometry optimization and frequency calculation, and the BS-II was used for evaluation of energy changes. Zero-point energy was evaluated with the DFT/BS-I method under assumption of harmonic oscillator. Solvation effects of benzene were evaluated with PCM method,⁶³ where the geometries were re-optimized in solution with the PCM method at the DFT/BS-I level. Free energies are evaluated at 25 °C according to the method of Whiteside.⁶⁴ Natural population analysis (NPA) is performed with the B3PW91/BS-II method.

All calculations were performed with Gaussian 03 program package.⁶⁵ NBO analysis is performed with NBO program 3.1.⁶⁶

Results and Discussion

The C-H activation of HBzq

The cross-coupling reaction of HBzq and benzene occurs through two separate C-H activation processes; one is the C-H activation of HBzq and the other is that of benzene. For brevity, the OAc ligand that finally changes to acetic acid (HOAc) is named OAc¹, and the other one that does not change in the reaction is OAc².

The C-H activation of HBzq by Pd(η^2 -OAc)₂ occurs through precursor complex (**PC**₁), transition state (**TS**₁) and intermediate Pd(Bzq)(η^2 -OAc)(HOAc) (**I**₁), as shown in Fig. 1. Geometrical features of these species are summarized, as follows: First, HBzq approaches the Pd complex to form **PC**₁. In **PC**₁, the C⁹-C¹⁰ double bond of HBzq coordinates to the Pd center in an η^2 -coordination way. The optimized Pd-C⁹ and Pd-C¹⁰ distances (2.25 Å) agree well with the experimental Pd-C distance of palladium-arene complexes (2.22 - 2.61 Å).⁶⁷ Another important geometrical change induced by the HBzq coordination is significantly large elongation of the Pd-OAc¹ bond (2.84 Å), indicating that the OAc¹ ligand changes to an η^1 -coordination form from an η^2 -coordination one; see Fig. 1. On the other hand, two Pd-O distances of OAc² little change. In other words, **PC**₁ is represented as Pd(η^1 -OAc¹)(η^2 -OAc²)(HBzq). This is because the η^2 -OAc ligand

must change to the η^1 -OAc ligand to supply one coordination site to HBzq. When going to **TS₁** from **PC₁**, the C-H bond of HBzq starts to be elongated. In **TS₁**, one imaginary frequency ($913.4i\text{ cm}^{-1}$) is observed, in which the H atom bound with the C^{10} atom is moving toward the O atom of OAc¹. This transition state is essentially the same as that of the C-H activation of benzene by $\text{Pd}(\eta^2\text{-O}_2\text{CH})_2$.⁵² After this transition state, the Pd-Ph bond and acetic acid (H-OAc^1) are formed in **I₁** as a result of heterolytic C-H activation by the Pd-OAc moiety. This acetic acid still interacts with the Pd center, as shown by the Pd-O bond distance (2.18\AA) which is a normal coordination bond distance. Essentially the same coordination of formic acid was reported in the C-H activation of benzene by $\text{Pd}(\eta^2\text{-O}_2\text{CH})_2$.⁵² After that, the acetic acid dissociates from the Pd center to afford the product **P₁**. **P₁** takes square planar geometry coordinated by Bzq and OAc².

Potential and Gibbs energy changes are evaluated by the DFT/BS-II and MP4(SDQ)/BS-II methods; see Fig. 2 for their values in benzene and see Fig. S1 for their values in gas phase. In this C-H activation step, the activation barrier (E_a) and the activation Gibbs energy change ($\Delta G^{0\dagger}$) correspond to the energy difference between **PC₁** and **TS₁**. The E_a value of this step in benzene is calculated to be 13.7 and 18.7 kcal/mol by the DFT and MP4(SDQ) methods, respectively, where the solvation effects of benzene are evaluated with the PCM method hereafter. The $\Delta G^{0\dagger}$ value in benzene is evaluated to be 10.5 and 15.5 kcal/mol by the DFT and MP4(SDQ) methods, respectively. The DFT method somewhat underestimates the E_a and $\Delta G^{0\dagger}$ values. These DFT- and MP4(SDQ)-calculated E_a values are similar to those of the C-H activation of benzene by $\text{Pd}(\eta^2\text{-O}_2\text{CH})_2$ which are 9.9 and 15.7 kcal/mol calculated by the DFT(B3LYP) and MP4(SDQ) methods, respectively.⁵² The MP4(SDQ)-calculated ΔE and ΔG^0 values are considerably negative, as shown in Fig. 2, where ΔE and ΔG^0 are defined as energy difference between the reactant (**R₁**) and the product (**P₁**) of this step. From these ΔE , E_a , ΔG^0 , and $\Delta G^{0\dagger}$ values, it is concluded that the C-H activation of HBzq easily occurs at experimental temperature ($130\text{ }^\circ\text{C}$).

Because the CCSD(T) method is computationally expensive and cannot be directly applied to our system, we employed the ONIOM method,⁶⁸ where the CCSD(T) and MP2 methods are used for

the important moiety and the whole system, respectively; the whole system is divided into the important moiety and the remaining moiety, as shown in Scheme S1. We found that ONIOM-calculated E_a value is essentially the same as the MP4(SDQ)-calculated value; see Fig. S5 and Table S1. From these results, we will present our discussion based on the MP4(SDQ)/BS-II computational results. The previous theoretical study by Sakaki and coworkers reported the similar results that the activation barrier converges when going from MP2 to MP4(SDQ) and the MP4(SDQ)-calculated E_a value is quite close to that of the CCSD(T)-calculated value.⁵²

For further understanding of the mechanistic details, changes in electron distribution by the reaction were investigated by natural population analysis (NPA), as shown in Fig. 3. Important features of the population changes are summarized, as follows: When going to **PC**₁ from **R**₁, the electron population of HBzq moderately decreases as a result of the coordination to Pd(η^2 -OAc)₂. However, the Pd atomic population decreases. On the other hand, the electron population of the OAc¹ ligand increases. These results indicate that the CT (charge transfer) from the OAc¹ ligand to the Pd center becomes weaker when going to **PC**₁ from **R**₁. This is because one of the O atoms of OAc¹ dissociates from the Pd center by the HBzq coordination; see above. In **TS**₁, the H atomic population considerably decreases but that of the C¹⁰ atom in the Bzq moiety considerably increases. These features suggest that the polarization of the C¹⁰-H bond occurs when going to **TS**₁ from **PC**₁; in other words, the H atom becomes positively charged but the C¹⁰ becomes negatively charged in **TS**₁. In **I**₁, the C¹⁰ atomic population considerably decreases, while that of Pd increases. This clearly shows that the CT from the C¹⁰ to the Pd center considerably occurs to form a new Pd-C¹⁰ bond.

The polarization of the C¹⁰-H bond in **TS**₁ is completely different from those of the oxidative addition mechanism, which are seen in the C-H activation catalyzed by Pt(PH)₃.^{35, 52, 53} This indicates that the C-H activation occurs in a heterolytic manner. These electron distribution changes can be interpreted in the same way as that of the theoretical study of the C-H activation of alkane by (Me₃SiO)₂Ti(=NSiMe₃)⁵³: i) The mixing between the C-H σ - and σ^* -type MOs (molecular orbitals) induces the polarization of the C-H bond to be broken. As a result, the C¹⁰ atom of the Bzq group

becomes negatively charged and the H atom becomes positively charged. ii) The CT from the negatively charged C¹⁰ atom to the Pd center stabilizes **TS₁** and contributes to the formation of new Pd-C¹⁰ bond. Also, the electrostatic stabilization is induced between the negatively charged C¹⁰ atom and the positively charged Pd center.

Benzoquinone coordination

As discussed above, the C-H activation of HBzq easily occurs from both kinetic and thermodynamic viewpoints. Because the product Pd(Bzq)(η^2 -OAc) **P₁** of the first C-H activation still has one OAc ligand, another C-H activation is possible.

According to the experimental findings,¹⁴ the arene cross-coupling occurs when BQ is added to the reaction system. Although it is widely proposed that BQ accelerates the RE (reductive elimination) step,⁶⁹ the role of BQ in the C-H activation process is unclear. Here, we investigated if BQ coordinates to Pd(Bzq)(η^2 -OAc) as experimentally proposed.¹⁴

We carried out geometry optimization of Pd(Bzq)(η^2 -OAc)(BQ) (**P₂**), as shown in Fig. 4. Frequency analysis showed that **P₂** is stable species in energy minimum. This coordination of BQ occurs via precursor complex (**PC₂**) and transition state (**TS₂**); see Fig. 4. In **P₂**, one Pd-O bond (2.35 Å) is somewhat longer than the other one (2.18 Å). But, even the longer Pd-O distance is close to the usual Pd-O coordinate bond distance. This suggests that the two Pd-O coordinate bonds are kept and the OAc forms distorted η^2 -coordinate bond unlike **PC₁** which contains the η^1 -OAc¹. Because of the presence of BQ, **P₂** is trigonal bipyramidal complex in which the Pd-C¹⁰ and shorter Pd-O bonds are in the axial position, as shown in Scheme 1 and Fig. 4.

Potential and Gibbs energy changes evaluated by the DFT and MP4(SDQ) methods are summarized in Fig. 5; for their values in gas phase, see Fig. S2. In the BQ coordination step, ΔE and ΔG^0 are defined as the potential and Gibbs energy differences between **R₂** and **P₂**, and E_a and $\Delta G^{0\ddagger}$ are defined as the potential and Gibbs energy differences of **PC₂** and **TS₂**. The E_a and ΔE values are calculated to be 6.7 and -13.2 kcal/mol, respectively, with the MP4(SDQ) method. The $\Delta G^{0\ddagger}$ and ΔG^0

values are calculated to be 8.7 and -1.7 kcal/mol, respectively, with the MP4(SDQ) method. These results indicate that BQ easily coordinates to the Pd complex. However, the DFT method considerably overestimates the $\Delta G^{0\ddagger}$ and ΔG^0 values. This is because the DFT method considerably underestimates the stabilization energy by the BQ coordination. The similar underestimation of coordination energy by the DFT was recently reported for the coordinate bonds of π -conjugate molecules with Pt and Pd complexes.⁷⁰

The electron distribution changes by the BQ coordination, as shown in Fig. 6. Since BQ is electron-deficient, the Pd atomic population decreases and the electron population of BQ increases by the BQ coordination. However, the electron populations of Bzq and OAc change less than those of BQ and Pd. These results indicate that the BQ coordination mainly induces electron re-distribution between BQ and Pd. In $\text{Pd}(\text{Bzq})(\eta^2\text{-OAc})$ **P₁** which is the product of the first C-H activation, the CT from the Bzq to the Pd occurs. As a result, the Pd atomic population increases by 0.20 e when going to **P₁** from $\text{Pd}(\eta^2\text{-OAc})_2$. This increase in the Pd atomic population would be unfavorable for the second C-H activation, because the metal center should be electrophilic for this type of C-H activation. From these viewpoints, it is expected that the BQ coordination is necessary for the second C-H activation process because the Pd atomic population decreases by the BQ coordination. This expectation will be investigated below in detail.

Second C-H activation and RE (Reductive Elimination) step

In this section, we investigated the reaction between benzene and $\text{Pd}(\text{Bzq})(\text{OAc})(\text{BQ})$ **P₂** which is the product of the second C-H activation.

As shown in Fig. 7, benzene approaches **P₂** at the opposite side of the BQ moiety to form precursor complex $\text{Pd}(\text{Bzq})(\text{OAc})(\text{BQ})(\text{C}_6\text{H}_6)$ **PC₃**. In **PC₃**, the Pd-benzene interaction is weaker than the Pd-HBzq interaction formed in the first C-H activation step, as indicated by the much longer Pd-C distance (4.42 Å); remember the Pd-C distance (2.25 Å) in **PC₁**. The C-H activation occurs through transition state **TS_{3a}** to afford intermediate $\text{Pd}(\text{Ph})(\text{Bzq})(\text{HOAc})(\text{BQ})$ **I₃**. In **TS_{3a}**, the C-H

bond of benzene is considerably elongated to 1.40 Å. Simultaneously, one Pd-O bond is elongated to 3.21 Å, indicating that η^2 -OAc turns into η^1 -OAc. In **I₃**, acetic acid is formed like the first C-H activation of HBzq, as shown in the optimized geometry of **I₃**. The Pd-O distance (2.31 Å) indicates that the acetic acid coordinates to the Pd center. Also, the Pd-C bond is formed at the axial position. Its bond distance (2.07 Å) is moderately longer than the Pd-C bond of Bzq (1.99 Å).

Starting from Pd(Bzq)(Ph)(HOAc)(BQ) **I₃**, the RE occurs through transition state **TS_{3b}** to afford product Pd(Bzq-Ph)(BQ)(HOAc) **P₃** (Bzq-Ph = 10-phenylbenzo[h]quinoline). In **TS_{3b}**, the C-C bond distance (2.10 Å) between Bzq and Ph becomes considerably shorter than that of **I₃** (2.63 Å). Another change to be noted is that the distance between the Pd and the O atom of OAc becomes considerably longer when going to **TS_{3b}** (2.57 Å) from **I₃** (2.31 Å). This indicates that the CT from the OAc ligand to the Pd center becomes weaker in **TS_{3b}**, because Pd(II) changes to Pd(0) in the RE step. In **P₃**, three important interactions are observed; i) Bzq-Ph coordinates to the Pd center through the phenyl moiety, ii) BQ coordinates to the Pd center in an η^2 -coordination way, and iii) HOAc weakly interacts with the Pd center by one O atom. Interestingly, the Pd-BQ interaction becomes stronger as indicated by the shorter Pd-C distances in **P₃** than in **TS_{3b}**. This is because the Pd center becomes more electron-rich after the RE; remember that BQ tends to form back-donation interaction because BQ is electron-deficient.

Potential and Gibbs energies are shown in Fig. 8; for these values in gas phase, see Fig. S3. The E_a and $\Delta G^{0\dagger}$ values of the second C-H activation are calculated to be 25.6 and 27.5 kcal/mol with the MP4(SDQ) method, where these values are defined as the energy difference between **PC₃** and **TS_{3a}**. Though these E_a and $\Delta G^{0\dagger}$ values are considerably larger than those of the first C-H activation of HBzq, these values are still moderate, indicating that the second C-H activation thermally occurs. If we concentrate on the RE after **I₃**, the E_a and $\Delta G^{0\dagger}$ values are calculated to be 1.1 and 0.4 kcal/mol, respectively, with the MP4(SDQ) method. These values clearly indicate that the RE easily occurs in a barrierless manner.

Compared to the MP4(SDQ) method, the DFT method tends to overestimate the E_a value

compared to the MP4(SDQ) method. However, the difference is moderate. On the other hand, the ΔE value is much different between these two methods, where the ΔE is defined as the potential energy difference between \mathbf{R}_3 and \mathbf{P}_3 ; the ΔE is calculated to be -10.8 kcal/mol by the DFT method and -23.5 kcal/mol by the MP4(SDQ) method; see Fig. 8. This is because the DFT method underestimates the stabilization energy by the BQ coordination compared with the MP4(SDQ) method, as discussed in the previous section and ref. 70.

The NBO populations change by the second C-H activation and RE steps, as shown in Fig. 9. When going to \mathbf{P}_3 from \mathbf{R}_3 , the Pd atomic population considerably increases and the H atomic population considerably decreases. Also, the electron population of the phenyl group considerably increases. These results are basically the same as those of the first C-H activation. Thus, the second C-H activation is understood to be the heterolytic type like the first C-H activation. In the RE, the Pd atomic population considerably increases expectedly, as shown in Fig. 9. Another important feature is that the electron population of BQ increases in \mathbf{P}_3 . This is because the Pd center changes into the Pd(0) in the RE and the BQ receives d electrons of Pd though the back-donation from the Pd to the BQ to stabilize \mathbf{TS}_{3b} and \mathbf{P}_3 . This reflects in the shortening of the Pd-BQ distance when going to \mathbf{P}_3 from \mathbf{I}_3 .

What role does benzoquinone play in this cross-coupling reaction?

As discussed above, the $\Delta G^{0\ddagger}$ for the BQ coordination is small and the ΔG^0 value is negative, indicating that BQ easily coordinates to Pd(η^2 -OAc)(Bzq). In this BQ coordination step, the η^2 -OAc ligand changes into the η^1 -OAc ligand to make a new coordination site for BQ. The η^1 -OAc form is also favorable for the second C-H activation because η^1 -OAc has a free O atom which easily abstracts the H atom of benzene. In addition to this geometrical feature, it is expected that the BQ coordination facilitates the second C-H activation from the viewpoint of electronic structure, as mentioned above.

For the further understanding of the role of BQ, the second C-H activation and the RE steps

without BQ are investigated here. First, the coordination of benzene to the product, $\text{Pd}(\text{Bzq})(\eta^2\text{-OAc})$ **R₂**, of the first C-H activation is examined. Like the BQ coordination to **P₂**, the coordination of benzene occurs through precursor complex (**PC₂'**) and transition state (**TS₂'**) to afford benzene complex $\text{Pd}(\text{Bzq})(\eta^2\text{-OAc})(\text{C}_6\text{H}_6)$ **P₂'**; see Fig. 10 for their optimized geometries. **P₂'** is square planar four-coordinate complex, as shown in Fig. 10. The largest difference in geometry between BQ and benzene coordinations is found in the coordinating position; BQ coordinates to the Pd center at the axial position to the Pd-Bzq-($\eta^2\text{-OAc}$) plane. On the other hand, benzene first approaches the Pd center from the axial direction but finally coordinates to the Pd center at the in-plane position; see Figs. 7 and 10.

After the benzene coordination, the C-H activation of benzene occurs through transition state (**TS_{3a}'**) to afford intermediate $\text{Pd}(\text{Bzq})(\text{Ph})(\text{HOAc})$ **I₃'**; see Fig. 10 for their optimized geometries. In **TS_{3a}'**, the C-H bond of benzene is considerably elongated (1.31 Å) compared to that of **P₂'** (1.09 Å). The structure of **I₃'** is significantly different from that of **I₃** which is formed in the presence of BQ; For instance, **I₃'** is square planar but **I₃** is trigonal bipyramidal. This is because the Pd(II) center takes d^8 electron configuration; note that the square planar structure is stable from the viewpoint of electronic structure, as well known, when four ligands coordinate to the d^8 metal.

Potential and Gibbs energy changes in the presence and absence of BQ are shown in Fig. 11; for their values in gas phase, see Fig. S4. The E_a and $\Delta G^{0\ddagger}$ values for the C-H activation of benzene are calculated to be 17.1 and 24.4 kcal/mol, respectively, by the MP4(SDQ) method, where the E_a and $\Delta G^{0\ddagger}$ values are defined as the energy difference between **TS_{3a}'** and **R₂** because **R₃** is less stable than **R₂**. This $\Delta G^{0\ddagger}$ value is almost the same as that (26.7 kcal/mol) of the second C-H activation process in the presence of BQ. The ΔG^0 of **I₃'** relative to **R₂** is moderate (7.4 kcal/mol). These computational results suggest that the C-H activation of benzene can occur even in the absence of BQ and that the BQ coordination little accelerates the second C-H activation against our expectation; see above.

After the formation of **I₃'**, the RE occurs to complete the catalytic reaction. The non-planar

transition state (**TS_{3b}'**) is optimized, as shown in Fig. 10. The $\Delta G^{0\ddagger}$ is calculated to be 34.7 kcal/mol with the MP4(SDQ)/BS-II method, which is much larger than that of the second C-H activation step. This is in contrast to the RE in the presence of BQ which occurs nearly barrierless. We also investigated another planar transition state in which the Ph and Bzq are on the Pd-N-O plane. However, the transition state could not be optimized; during the geometry optimization, the phenyl group deviates from the Pd-N-O plane and finally the same transition state as **TS_{3b}'** is presented. The non-planar transition state of the RE is not surprising; it was reported and the reason was discussed previously.⁷¹

It is of considerable importance to clarify the reason why the $\Delta G^{0\ddagger}$ and ΔG^0 values of the RE are very large in the absence of BQ; the $\Delta G^{0\ddagger}$ and ΔG^0 values are 0.4 and -18.5 kcal/mol in the presence of BQ but 34.7 and 8.7 kcal/mol in the absence of BQ, where $\Delta G^{0\ddagger}$ and ΔG^0 are defined as the Gibbs energy difference between **I₃** (or **I₃'**) and **TS_{3b}** (or **TS_{3b}'**) and that between **I₃** (or **I₃'**) and the product complex **P₃** (or **P₃'**), respectively, because we concentrate here on the RE. These results clearly indicate that BQ stabilizes the transition state and the product of the RE. One reason for this result is clear from the structures of **I₃'** and **TS_{3b}'**; because the phenyl group is on the Pd-Bzq-OAc plane in **I₃'**, the phenyl group must considerably move from the Pd-Bzq-OAc plane toward Bzq in **TS_{3b}'**, as shown in Fig. 10. As a result, **TS_{3b}'** is energetically unfavorable compared with **I₃'**, leading to the large $\Delta G^{0\ddagger}$ value. On the other hand, the phenyl group does not need to move very much when going to **TS_{3b}** from **I₃** in the presence of BQ, as shown in Fig. 7, because the phenyl group takes the axial position in **I₃** and the geometry of **I₃** resembles well that of **TS_{3b}**. In other words, the BQ coordination leads to the formation of five-coordinated trigonal bipyramidal intermediate in which the phenyl group takes the favorable position for the RE.

Another reason is the CT from the Pd to the BQ, as follows: In the presence of BQ, the Pd atomic population is +0.69 e in **TS_{3b}** and +0.45 e in **P₃**, while it is +0.36 e in **TS_{3b}'** and +0.32 e in **P₃'**. Consistent with these differences in the Pd atomic population, the population of BQ increases by 0.10 e during the RE step when going to **P₃** from **I₃**; see Fig. 9. These population changes are

induced by the CT from the Pd to the BQ in **TS_{3b}** and **P₃**. Not only population changes but also the geometry of **P₃** supports this CT; in **P₃**, the C=C bond of the BQ moiety is moderately elongated (1.42 Å) compared with that of **I₃** (1.40 Å).

From these computational results, it should be clearly concluded that the BQ coordination with the Pd center leads to the smaller $\Delta G^{0\ddagger}$ and more negative ΔG^0 of the RE than those in absence of BQ; in other words, the arene-arene cross-coupling reaction easily occurs in the presence of BQ because the RE step is accelerated by BQ.

Conclusions

The synthetically useful arene cross-coupling reaction catalyzed by Pd(OAc)₂ was theoretically studied with the DFT, MP2 to MP4(SDQ), and CCSD(T) methods. BQ is experimentally reported to be necessary for this cross-coupling reaction. Our computational study elucidated the whole mechanism of this arene cross-coupling reaction and the role of BQ.

In this reaction, two C-H activations occur independently. The first is the C-H activation of HBzq, which leads to the formation of Pd(Bzq)(η^2 -OAc). This process is understood in terms of heterolytic type C-H activation unlike the oxidative addition type C-H activation.²⁶ BQ easily coordinates to Pd(Bzq)(η^2 -OAc) to induce distortion of the Pd(II) complex from the square planar structure to the trigonal bipyramidal one. The coordinate bond is formed by the CT from the Pd to the BQ. This complex Pd(Bzq)(η^2 -OAc)(BQ) is as stable as the square planar Pd(Bzq)(η^2 -OAc). Both E_a and $\Delta G^{0\ddagger}$ are small for the BQ coordination step, indicating this step easily occurs. Then, the C-H activation of benzene occurs with $\Delta G^{0\ddagger}$ value of 27.5 kcal/mol to afford the intermediate (**I₃**). Finally, the RE readily occurs with nearly no barrier; $\Delta G^{0\ddagger}$ for this step is quite small (0.4 kcal/mol). These computational results suggest that the rate-determining step is the C-H activation of benzene by Pd(Bzq)(η^2 -OAc)(BQ).

To clarify the role of BQ, we investigated the cross-coupling reaction of HBzq and benzene in

the absence of BQ. The first step is the C-H activation of HBzq which is the same as that in the presence of BQ. After that, benzene coordinates to the Pd center to form $\text{Pd}(\text{Bzq})(\eta^2\text{-OAc})(\text{C}_6\text{H}_6)$ (\mathbf{P}_2'). The $\Delta G^{0\ddagger}$ for this step is moderate (15.0 kcal/mol), indicating the coordination of benzene easily occurs. Starting from \mathbf{P}_2' , the C-H activation of benzene occurs via transition state \mathbf{TS}_{3a}' to afford intermediate \mathbf{I}_3' . Then, the RE of Bzq-Ph occurs via non-planar transition state \mathbf{TS}_{3b}' to afford the product complex $\text{Pd}(\text{Bzq-Ph})(\text{HOAc})$ \mathbf{P}_3' (Bzq-Ph = 10-phenylbenzo[*h*]quinoline). The greatest difference from the reaction in the presence of BQ is observed in the structure of \mathbf{I}_3' ; in the absence of BQ, the phenyl group is on the Pd-Bzq-HOAc plane in \mathbf{I}_3' in contrast to \mathbf{I}_3 in which the phenyl group takes the axial position. As a result, the RE step in the absence of BQ occurs with quite large geometry changes, but the RE occurs with moderate geometry changes in the presence of BQ. In addition to the smaller geometry changes, BQ stabilizes \mathbf{TS}_{3b} and \mathbf{P}_3 by the back-donation from Pd(0) to BQ. Actually, the considerably large difference is observed in $\Delta G^{0\ddagger}$ and ΔG^0 of the RE step; in the presence of BQ, the $\Delta G^{0\ddagger}$ and ΔG^0 are 0.4 and -18.5 kcal/mol, respectively, while in the absence of BQ, the $\Delta G^{0\ddagger}$ and ΔG^0 are 34.7 and 8.7 kcal/mol, respectively.

Our theoretical study clearly shows that BQ plays very important role in the RE step to accelerate the arene-arene cross-coupling reaction. We believe that the new insight found in this work is valuable for further development of the C-H activation and the cross-coupling reaction of arenes.

Acknowledgements

This work was financially supported by Grand-in-Aids on basis research (No. 1530012), Priority Areas for “Molecular Theory for Real Systems” (No. 461), and NAREGI Project from the Ministry of Education, Science, Sports, and Culture. Some of theoretical calculations were performed with

SGI workstations of Institute for Molecular Science (Okazaki, Japan), and some of them were carried out with PC cluster computers in our laboratory.

Notes and references

- 1 F. Diederich, in *Metal Catalyzed Cross-Coupling Reactions*, ed. A. de Mejiere, John Wiley & Sons, New York, 2004.
- 2 A. E. Shilov, in *Activation of Saturated Hydrocarbons by Transition Metal Complexes*, D. Reidel, Boston, MA, 1984.
- 3 R. H. Crabtree, *Chem. Rev.* 1985, **85**, 245.
- 4 A. D. Ryabov, *Chem. Rev.* 1990, **90**, 403.
- 5 A. E. Shilov and B. G. Shulpin, *Chem. Rev.* 1997, **97**, 2879.
- 6 A. R. Dick and M. S. Sanford, *Tetrahedron* 2006, **62**, 2439
- 7 J. A. Labinger and J. E. Bercaw, *Nature* 2002, **417**, 507
- 8 B.-J. Li, S.-D. Yang and Z.-J. Shi, *Synlett* 2008, **7**, 949
- 9 J. C. Lewis, R. G. Bergman and J. A. Ellman, *Acc. Chem. Res.* 2008, **41**, 1013
- 10 M. Catellani, E. Motti, N. D. Ca' and R. Ferraccioli, *Eur. J. Org. Chem.* 2007, 4153
- 11 D. J. Cardenas, *Angew. Chem., Int. Ed.* 2003, **42**, 384
- 12 R. Li, L. Jiang and W. Lu, *Organometallics* 2006, **25**, 5973
- 13 (a) J. K. Stille, *Angew. Chem., Int. Ed.* 1986, **25**, 508. (b) P. Epsinet and A. M. Echavarren, *Angew. Chem., Int. Ed.* 2004, **43**, 4704.
- 14 (a) A. Suzuki, *Pure Appl. Chem.* 1994, **66**, 213. (b) N. Miyaura and A. Suzuki, *Chem. Rev.* 1995, **95**, 2457. (c) A. F. Indolese, *Tetrahedron Lett.* 1997, **38**, 3513. (d) S. Kotha, K. Lahiri and D. Kashinath, *Tetrahedron* 2002, **58**, 9633. (e) N. Miyaura, *Top. Curr. Chem.* 2002, **219**, 11.
- 15 (a) R. Mas-Balleste and L. Que Jr., *Science*, 2006, **312**, 1885. (b) M. S. Chen and M. C. White, *Science*, 2007, **318**, 783
- 16 (a) E. M. Beck, R. Hatley and M. J. Gaunt, *Angew. Chem., Int. Ed.* 2008, **47**, 3004. (b) R. G. Bedford and M. Betham, *J. Org. Chem.* 2006, **71**, 9403. (c) K. Chen, J. M. Richter and P. S. Baran, *J. Am. Chem. Soc.* 2008, **130**, 7247. (d) M. Christmann, *Angew. Chem., Int. Ed.* 2008, **47**, 2740. (e) X. Dai, Z. L. Wan, R. G. Kerr and H. M. L. Davies, *J. Org. Chem.* 2007, **72**, 1895. (f) H. M. L. Davies

- and X. Dai, *Tetrahedron* 2006, **62**, 10477. (g) H. M. L. Davies, X. Dai and M. S. Long, *J. Am. Chem. Soc.* 2006, **128**, 2485. (h) R. Giri and J. Q. Yu, *J. Am. Chem. Soc.* 2008, **130**, 14082. (i) P. Kocovsky, V. Dunn, A. Gogoll and V. Langer, *J. Org. Chem.* 1999, **64**, 101. (j) B. J. Li, S. D. Yang and Z. J. Shi, *Synlett* 2008, 949. (k) K. C. Nicolaou, P. G. Bulger and D. Sarlah, *Angew. Chem., Int. Ed.* 2005, **44**, 4442. (l) J. C. Torres, A. C. Pinto and S. J. Garden, *Tetrahedron* 2004, **60**, 9889. (m) A. S. Tsai, R. G. Bergman and J. A. Ellman, *J. Am. Chem. Soc.* 2008, **130**, 6316. (n) C. Verrier, T. Martin, C. Hoarau and F. Marsais, *J. Org. Chem.* 2008, **73**, 7383.
- 17 G. Dyker, *Angew. Chem., Int. Ed.* 1999, **38**, 1698.
- 18 V. Ritleng, C. Sirlin and M. Pfeffer, *Chem. Rev.* 2002, **102**, 1731.
- 19 F. Kakiuchi and N. Chatani, *Adv. Synth. Catal.* 2003, **345**, 1077.
- 20 D. Alberico, M. E. Scott and M. Lautens, *Chem. Rev.* 2007, **107**, 174.
- 21 H. A. Burton and I. V. Kozhevnikov, *J. Mol. Catal. A* 2002, **185**, 285
- 22 M. Takahashi, K. Masui, H. Sekiguchi, N. Kobayashi, A. Mori, M. Funahashi and N. Tamaoki, *J. Am. Chem. Soc.* 2006, **128**, 10930
- 23 K. L. Hull, E. L. Lanni and M. S. Sanford, *J. Am. Chem. Soc.* 2006, **128**, 14047
- 24 X. L. Li, J. B. Hewgley, C. A. Mulrooney, J. M. Yang and M. C. Kozlowski, *J. Org. Chem.* 2003, **68**, 5500
- 25 F. Faccini, E. Motti and M. Catellani, *J. Am. Chem. Soc.* 2004, **126**, 78
- 26 D. J. Cardenas, B. Martin-Matute and A. M. Echavarren, *J. Am. Chem. Soc.* 2006, **128**, 5033
- 27 D. R. Stuart and K. Fagnou, *Science* 2007, **316**, 1172
- 28 (a) S. Murai, F. Kakiuchi, S. Sekine, Y. Tanaka, A. Kamatani, M. Sonoda and N. Chatani, *Nature* 1993, **366**, 529. (b) S. Murai, F. Kakiuchi, S. Sekine, Y. Tanaka, A. Kamatani, M. Sonoda and N. Chatani, *Pure Appl. Chem.* 1994, **66**, 1527. (c) F. Kakiuchi, S. Sekine, Y. Tanaka, A. Kamatani, M. Sonoda, N. Chatani and S. Murai, *Bull. Chem. Soc. Jpn.* 1995, **68**, 62. (d) S. Murai, N. Chatani and F. Kakiuchi, *Pure Appl. Chem.* 1997, **69**, 589. (e) N. Chatani, T. Morimoto, Y. Fukumoto and S. Murai, *J. Am. Chem. Soc.* 1998, **120**, 5335.

- 29 T. Matsubara, N. Koga, D. G. Musaev and K. Morokuma, *J. Am. Chem. Soc.* 1998, **120**, 12692
- 30 K. K. Hull and M. S. Sanford, *J. Am. Chem. Soc.* 2007, **129**, 11904
- 31 X. Chen, J.-J. Li, X.-S. Hao, C. E. Goodhue and J.-Q. Yu, *J. Am. Chem. Soc.* 2006, **128**, 78
- 32 (a) A. C. Albeniz, P. Epsinet and B. Martin-Ruiz, *Chem. –Eur. J.* 2001, **7**, 2481. (b) J.-E. Backvall, S. E. Bystrom and R. E. Nordberg, *J. Org. Chem.* 1984, **49**, 4619
- 33 J.-Y. Saillard and R. Hoffmann, *J. Am. Chem. Soc.* 1984, **106**, 2006.
- 34 (a) S. Obara, K. Kitaura and K. Morokuma, *J. Am. Chem. Soc.* 1984, **106**, 7482. (b) N. Koga and K. Morokuma, *J. Am. Chem. Soc.* 1990, **94**, 5454. (c) N. Koga and K. Morokuma, *J. Am. Chem. Soc.* 1993, **115**, 6883.
- 35 (a) J. J. Low and W. A. Goddard, *J. Am. Chem. Soc.* 1986, **108**, 6115. (b) J. J. Low and W. A. Goddard, *Organometallics* 1986, **5**, 609.
- 36 (a) M. R. A. Blomberg, P. E. M. Siegbahn, U. Nagashima and J. Wennerberg, *J. Am. Chem. Soc.* 1991, **113**, 424. (b) M. Svensson, M. R. A. Blomberg and P. E. M. Siegbahn, *J. Am. Chem. Soc.* 1991, **113**, 7076. (c) M. R. A. Blomberg, P. E. M. Siegbahn and M. Svensson, *J. Am. Chem. Soc.* 1992, **114**, 6095. (d) P. E. M. Siegbahn, M. R. A. Blomberg and M. Svensson, *J. Am. Chem. Soc.* 1993, **115**, 4191. (e) M. R. A. Blomberg, P. E. M. Siegbahn and M. Svensson, *J. Phys. Chem.* 1994, **98**, 2062. (f) P. E. M. Siegbahn and M. R. A. Blomberg, *Organometallics* 1994, **13**, 354. (g) P. E. M. Siegbahn, *Organometallics* 1994, **13**, 2833. (h) P. E. M. Siegbahn and M. Svensson, *J. Am. Chem. Soc.* 1994, **116**, 10124. (i) P. E. M. Siegbahn, *J. Am. Chem. Soc.* 1996, **118**, 1487. (j) P. E. M. Siegbahn and R. H. Carbtree, *J. Am. Chem. Soc.* 1996, **118**, 4442.
- 37 (a) J. Song and M. B. Hall, *Organometallics* 1993, **12**, 3118. (b) R. Jimenez-Catao and M. B. Hall, *Organometallics* 1996, **15**, 1889. (c) S.-Q. Niu and M. B. Hall, *J. Am. Chem. Soc.* 1998, **120**, 6169.
- 38 (a) S. Sakaki and M. Ieki, *J. Am. Chem. Soc.* 1993, **115**, 2373. (b) S. Sakaki, B. Biswas and M. Sugimoto, *J. Chem. Soc., Dalton Trans.* 1997, 803. (c) S. Sakaki, B. Biswas and M. Sugimoto,

Organometallics 1998, **17**, 1278.

- 39 C. Hinderling, D. Feichtinger, D. A. Plattner and P. Chen, *J. Am. Chem. Soc.* 1997, **119**, 10793.
- 40 M.-D. Su and S.-Y. Chu, *J. Am. Chem. Soc.* 1997, **119**, 5373.
- 41 J. Espinosa-Garcia, J. C. Corchado and D. G. Truhlar, *J. Am. Chem. Soc.* 1997, **119**, 9891.
- 42 (a) K. Yoshizawa, T. Ohta, T. Yamabe, R. Hoffmann, *J. Am. Chem. Soc.* 1997, **119**, 12311.
(b) K. Yoshizawa, Y. Shiota and T. Yamabe, *J. Am. Chem. Soc.* 1998, **120**, 564. (c) K. Yoshizawa, Y. Shiota and T. Yamabe, *J. Am. Chem. Soc.* 1998, **121**, 147.
- 43 K. Mylvaganam, G. B. Bacskay and N. S. Hush, *J. Am. Chem. Soc.* 1999, **121**, 4633.
- 44 I. P. Beletskaya, A. G. Bessmertnykh and R. Guilard, *Tetrahedron Lett.* 1999, **40**, 6393.
- 45 B. Gotov, J. Kaufmann, H. Schumann and H. G. Schmalz, *Synlett* 2002, 361.
- 46 H. Schumann, J. Kaufmann, H. G. Schmalz, A. Bottcher and B. Gotov, *Synlett* 2003, 1783.
- 47 L. J. Ackerman, J. P. Sadighi, D. M. Kurtz, J. A. Labinger and J. E. Bercaw, *Organometallics* 2003, **22**, 3884.
- 48 D. Prim, B. Andrioletti, F. Rose-Munch, E. Rose and F. Couty, *Tetrahedron* 2004, **60**, 3325.
- 49 U. Christmann, D. A. Pantazis, J. Benet-Buchholz, J. E. McGrady, F. Maseras and R. Vilar, *Organometallics* 2006, **25**, 5990.
- 50 S. H. Cho, S. J. Hwang and S. Chang, *J. Am. Chem. Soc.* 2008, **130**, 9254.
- 51 Y. Fu, Z. Li, S. Liang, Q. X. Guo and L. Liu, *Organometallics* 2008, **27**, 3736.
- 52 B. Biswas, M. Sugimoto and S. Sakaki, *Organometallics*, 2000, **19**, 3895.
- 53 N. Ochi, Y. Nakao, H. Sato and S. Sakaki, *J. Am. Chem. Soc.* 2007, **129**, 8615.
- 54 M. Lafarance, C. N. Rowley, T. K. Woo and K. Fagnou, *J. Am. Chem. Soc.* 2006, **128**, 8754.
- 55 I. Ozdemir, S. Demir, B. Cetinkaya, G. Gourlaouen, F. Maseras, C. Bruneau and P. H. Dixneuf, *J. Am. Chem. Soc.* 2008, **130**, 1156.
- 56 A. D. Becke, *Phys. Rev. A* 1988, **38**, 3098.
- 57 J. P. Perdew, J. A. Chevary, S. H. Vosko, K. A. Jackson, M. R. Pederson, D. J. Singh and C.

Fiolhais, *Phys. Rev. B*, 1992, **46**, 6671.

58 J. P. Perdew, K. Burke and Y. Wang, *Phys. Rev. B* 1996, **54**, 16533.

59 P. J. Hay and W. R. Wadt, *J. Chem. Phys.* 1985, **82**, 270.

60 R. Ditchfield, W. J. Hehre and J. A. Pople, *J. Chem. Phys.* 1971, **54**, 724.

61 D. Andrae, U. Haussermann, M. Dolg, H. Stoll and H. Preuss, *Theor. Chem. Acta.* 1990, **77**, 123.

62 T. H. Dunning Jr., *J. Chem. Phys.* 1989, **90**, 1007.

63 S. Miertus, E. Scrocco and J. Tomasi, *Chem. Phys.* 1981, **55**, 117.

64 M. Mammen, E. I. Shakhnovich, J. M. Deutch and G. M. Whitesides, *J. Org. Chem.* 1998, **63**, 3821.

65 J. A. Pople, *et al. Gaussian 03, ReVision C.02*, Gaussian: Inc.:Wallingford, CT, 2004.

66 J. E. Carpenter and F. Weinhold, *J. Mol. Struct. (Theochem)*, 1988, **169**, 41.

67 M. Catellani, C. Mealli, E. Motti, P. Paoli, E. Perez-Carreno and P. S. Pregosin, *J. Am. Chem. Soc.* 2002, **124**, 4336.

68 (a) F. Maseras and K. Morokuma, *J. Comp. Chem.* 1995, **16**, 1170 (b) S. Humbel, S. Sieber and K. Morokuma, *J. Chem. Phys.* 1996, **105**, 1959. (c) T. Matsubara, S. Sieber and K. Morokuma, *Int. J. Quant. Chem.* 1996, **60**, 1101. (d) M. Svensson, S. Humbel, R. D. J. Froese, T. Matsubara, S. Sieber and K. Morokuma, *J. Phys. Chem.* 1996, **100**, 19357. (e) M. Svensson, S. Humbel and K. Morokuma, *J. Chem. Phys.* 1996, **105**, 3654. (f) S. Dapprich, I. Komaromi, K. S. Byun, K. Morokuma and M. J. Frisch, *J. Mol. Struct. (Theochem)*, 1999, **462**, 1. (g) T. Vreven and K. Morokuma, *J. Comp. Chem.* 2000, **21**, 1419. (h) S. Sakaki, N. Mizoe and M. Sugimoto, *Organometallics*, 1998, **17**, 2510.

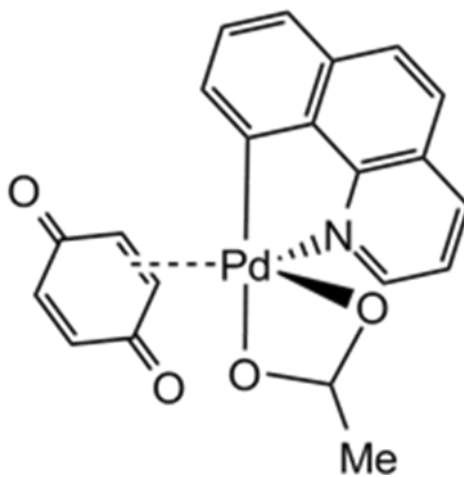
69 (a) F. Ozawa, T. Hikida and T. Hayashi, *J. Am. Chem. Soc.* 1994, **116**, 2844 (b) A. C. Albeniz, P. Epsinet and B. Martin-Ruiz, *Chem. Eur. J.* 2001, **7**, 2483.

70 (a) Y. Kamenno, A. Ikeda, Y. Nakao, H. Sato and S. Sakaki, *J. Phys. Chem. A*, 2005, **109**, 8055. (b) A. Ikeda, Y. Kamenno, Y. Nakao, H. Sato and S. Sakaki, *J. Organomet. Chem.* 2007, **692**,

299. (c) A. Ikeda, Y. Nakao, H. Sato and S. Sakaki, *J. Phys. Chem. A*, 2007, **111**, 7142.

71 S. Sakaki, N. Mizoe, Y. Musashi, B. Biswas and M. Sugimoto, *J. Phys. Chem. A*, 1998, **102**,
8027.

Scheme and figures



Scheme 1

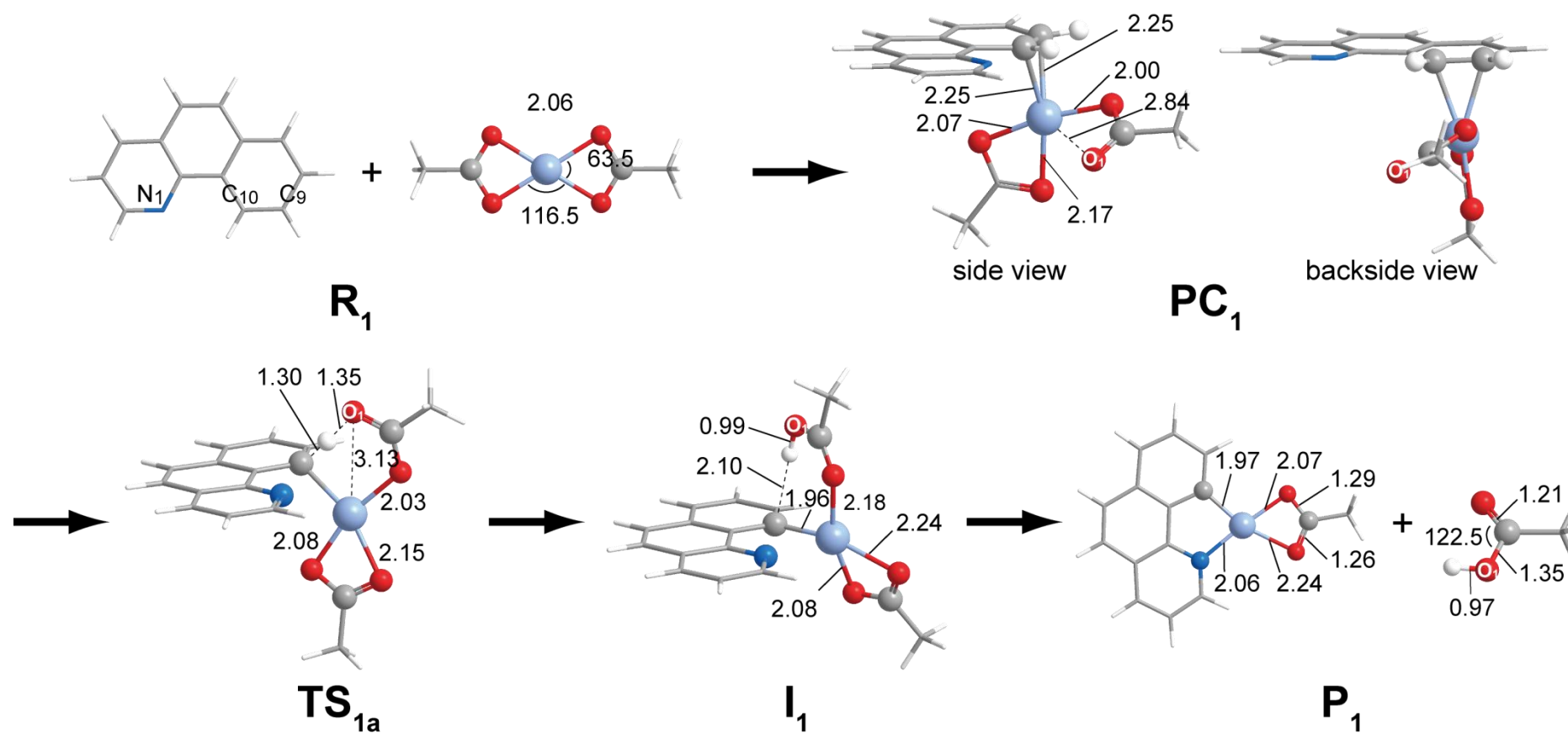


Fig. 1. Geometry changes in the C-H activation of HBzq by $\text{Pd}(\text{OAc})_2$. Bond lengths are in Å and bond angle are in degrees

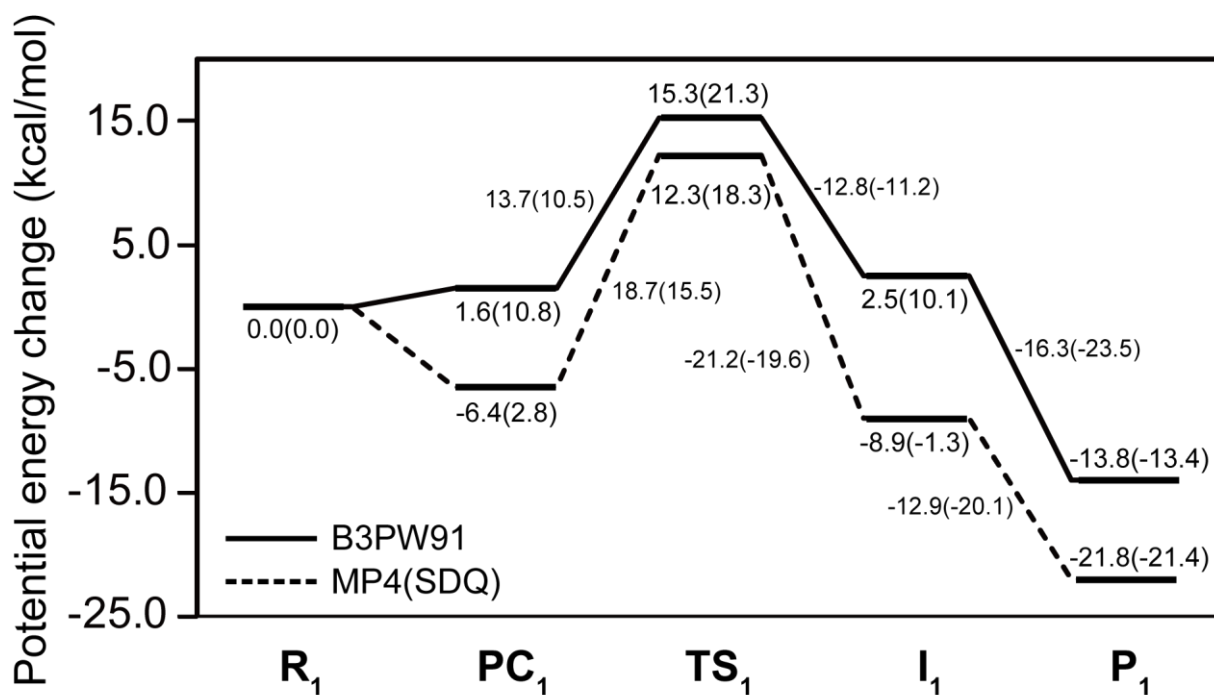


Fig. 2. Potential energy changes for the C-H activation of HBzq by Pd(OAc)₂ in benzene. Energies^{a)} are given in kcal/mol unit. ^{a)} In parentheses are Gibbs free energy changes.

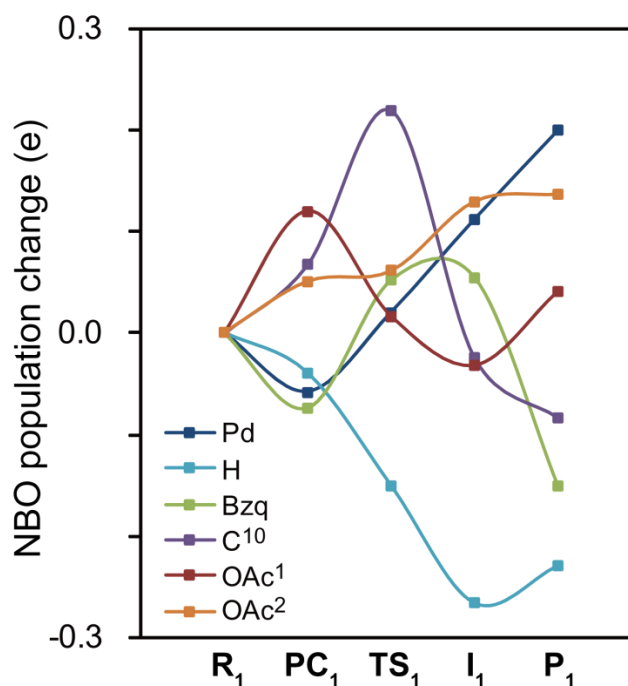


Fig. 3. Population changes^{a)} for the C-H activation of HBzq by Pd(OAc)₂. A positive value represents increase in population relative to R₁, and vice versa. ^{a)} DFT/BS-II level was employed.

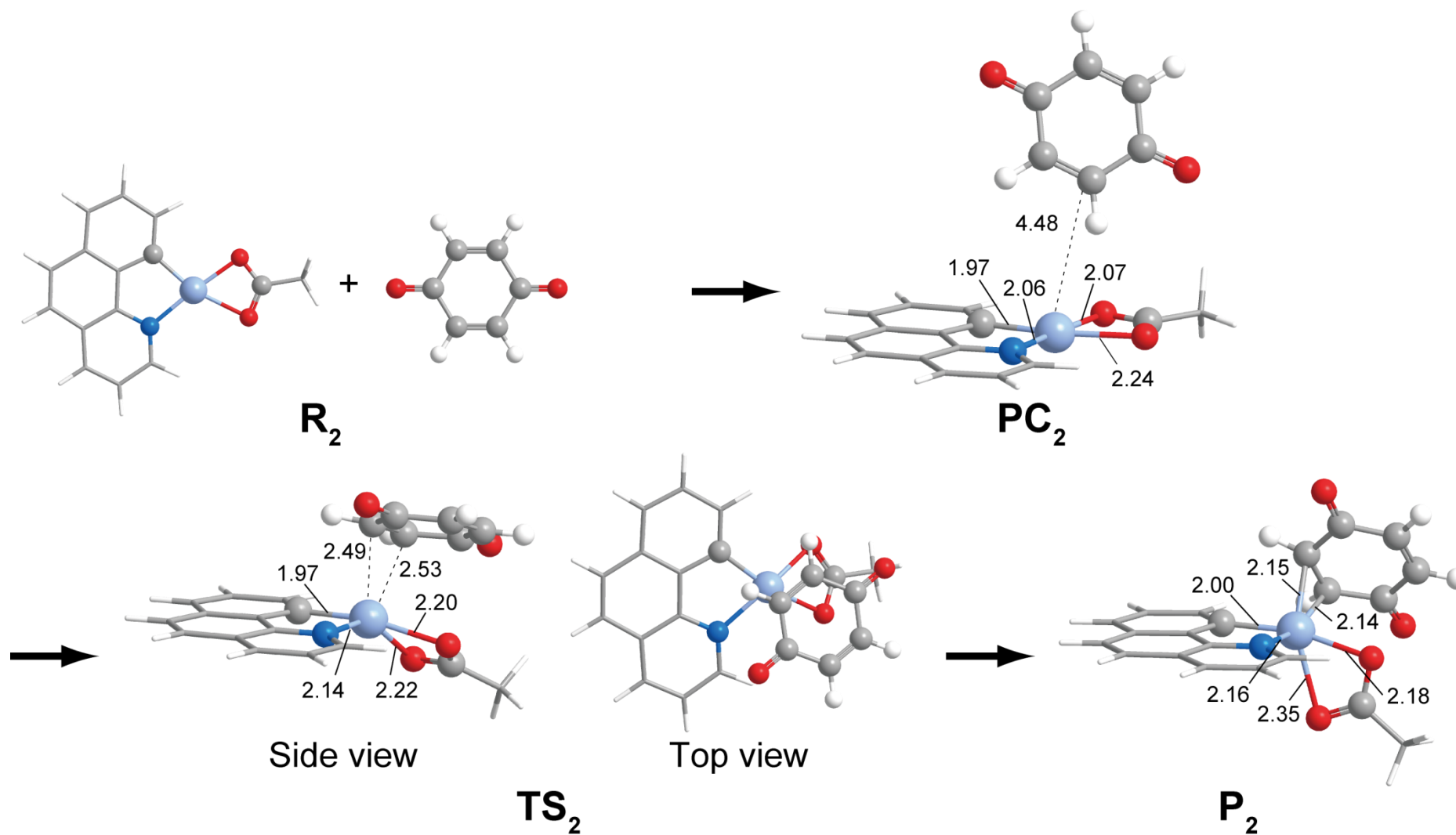


Fig. 4. Geometry changes in the BQ coordination to $\text{Pd}(\text{Bzq})(\text{OAc})$. Bond lengths are in Å and bond angle are in degrees.

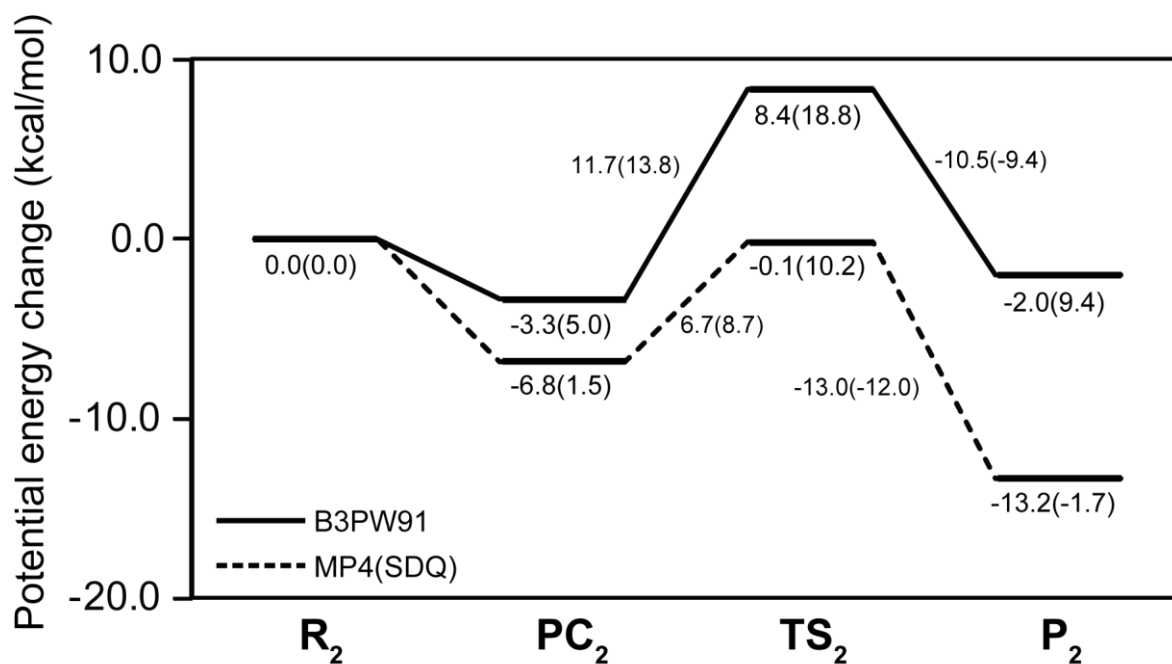


Fig. 5. Potential energy changes for the BQ coordination to Pd(Bzq)(OAc) in benzene. Energies^{a)} are given in kcal/mol unit. ^{a)} In parentheses are Gibbs free energy changes.

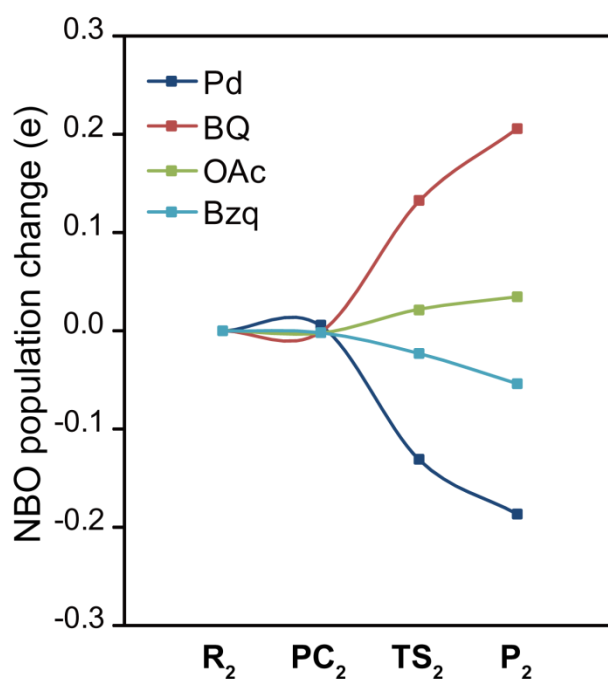


Fig. 6. Population changes^{a)} for the BQ coordination to Pd(Bzq)(OAc). A positive value represents increase in population relative to R_2 , and vice versa. ^{a)} DFT/BS-II level was employed.

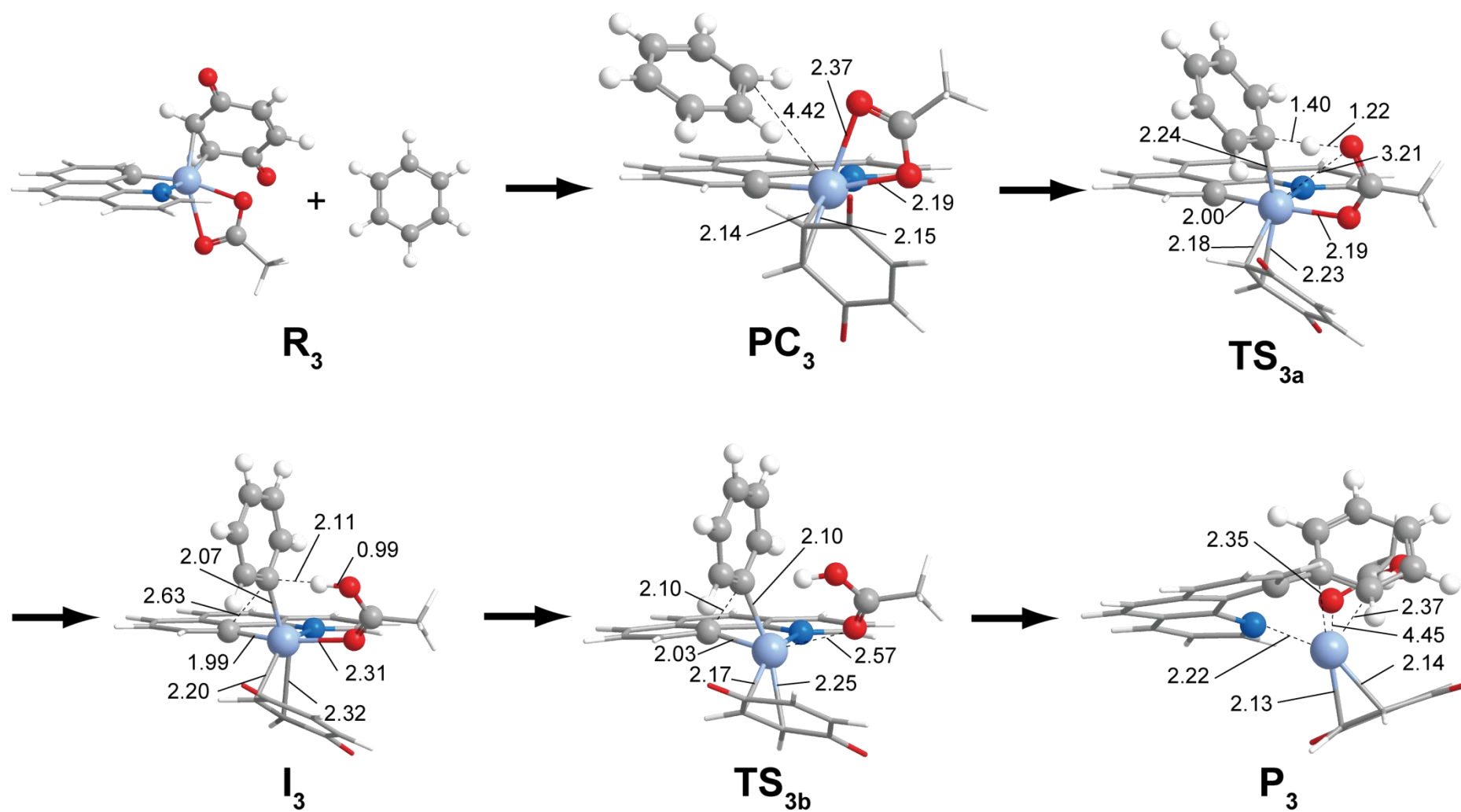


Fig. 7. Geometry changes in the C-H activation of benzene by $\text{Pd}(\text{Bzq})(\text{OAc})(\text{BQ})$. Bond lengths are in Å and bond angle are in degrees.

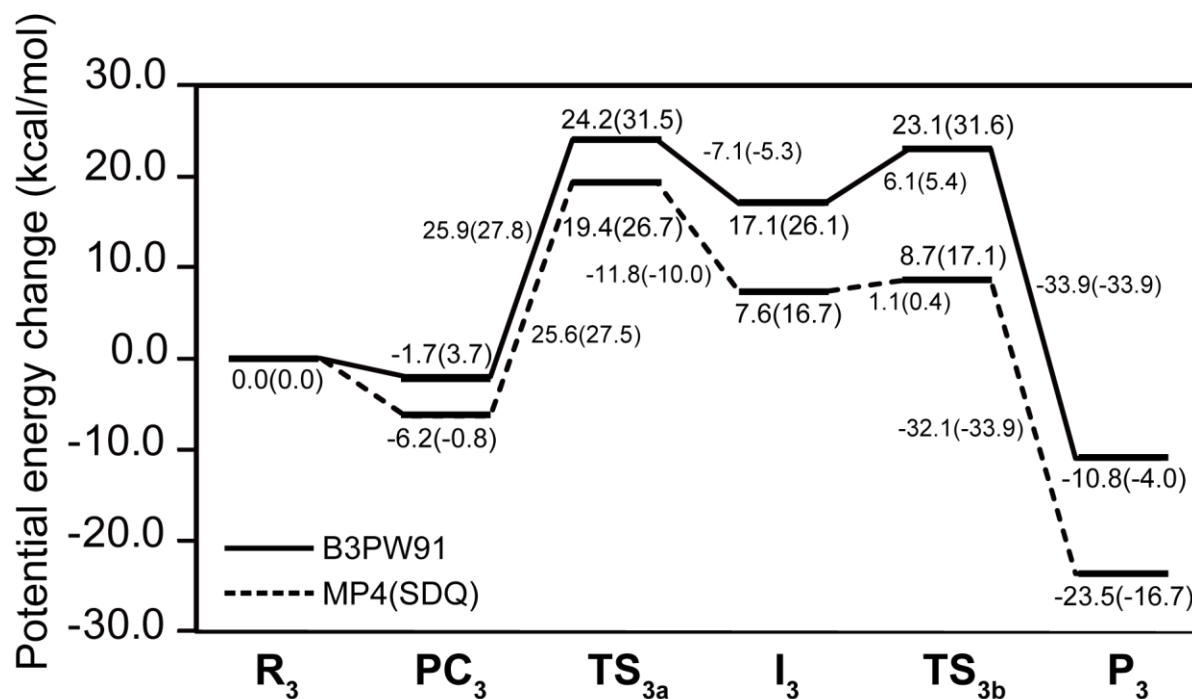


Fig. 8. Potential energy changes for the C-H activation of benzene by Pd(Bzq)(OAc)(BQ) in benzene. Energies^{a)} are given in kcal/mol unit. ^{a)} In parentheses are Gibbs free energy changes.

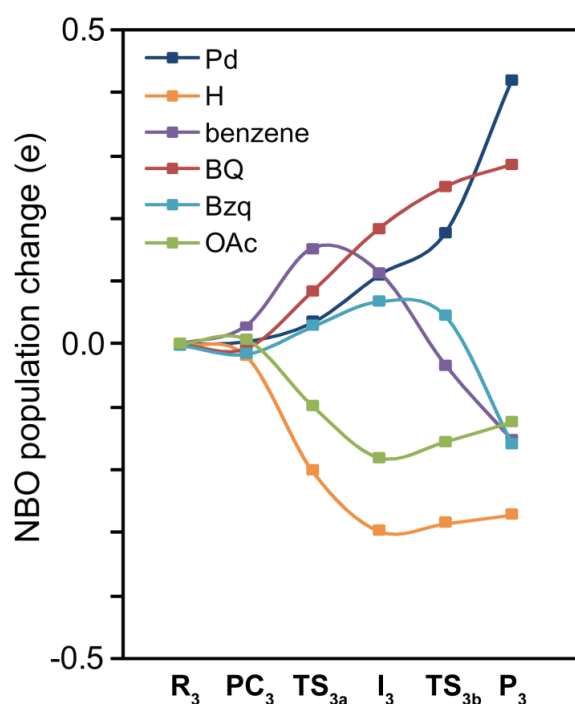


Fig. 9. Population changes^{a)} for the C-H activation of benzene by Pd(Bzq)(OAc)(BQ). A positive value represents increase in population relative to R₃, and vice versa. ^{a)} DFT/BS-II level was employed.

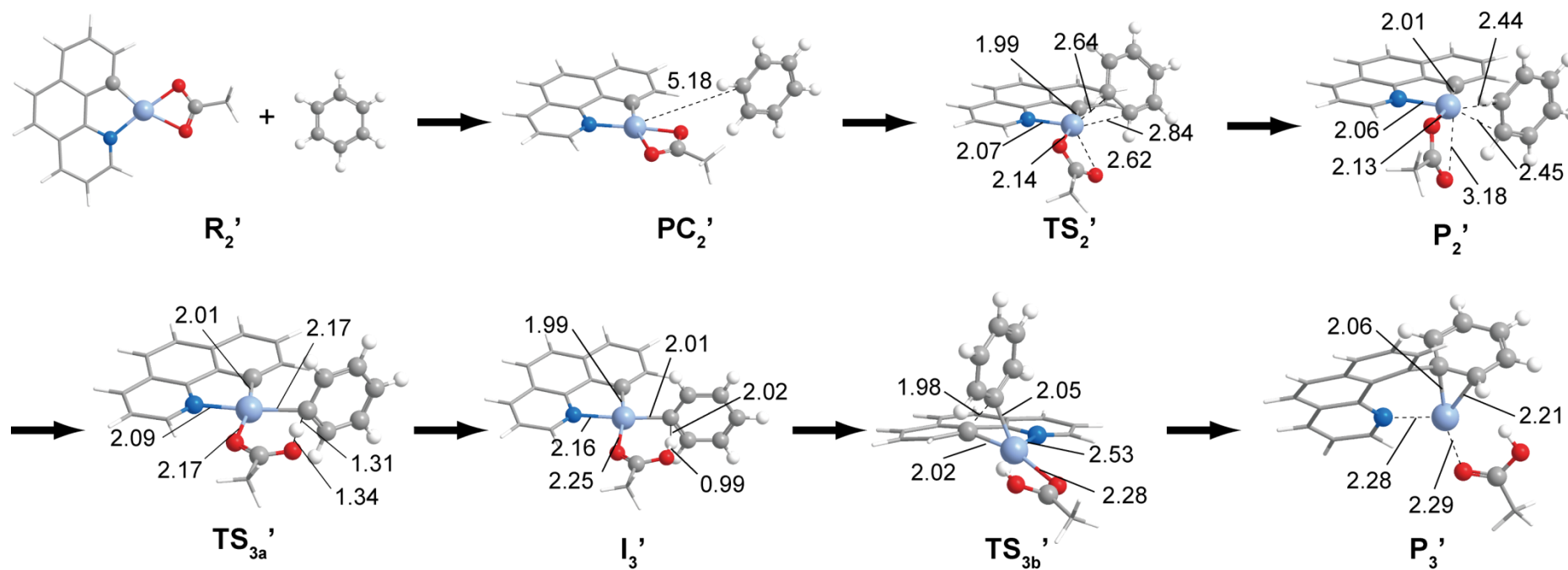


Fig. 10. Geometry changes in the C-H activation of benzene by $\text{Pd}(\text{Bzq})(\text{OAc})$ in the absence of BQ. Bond lengths are in Å and bond angle are in degrees.

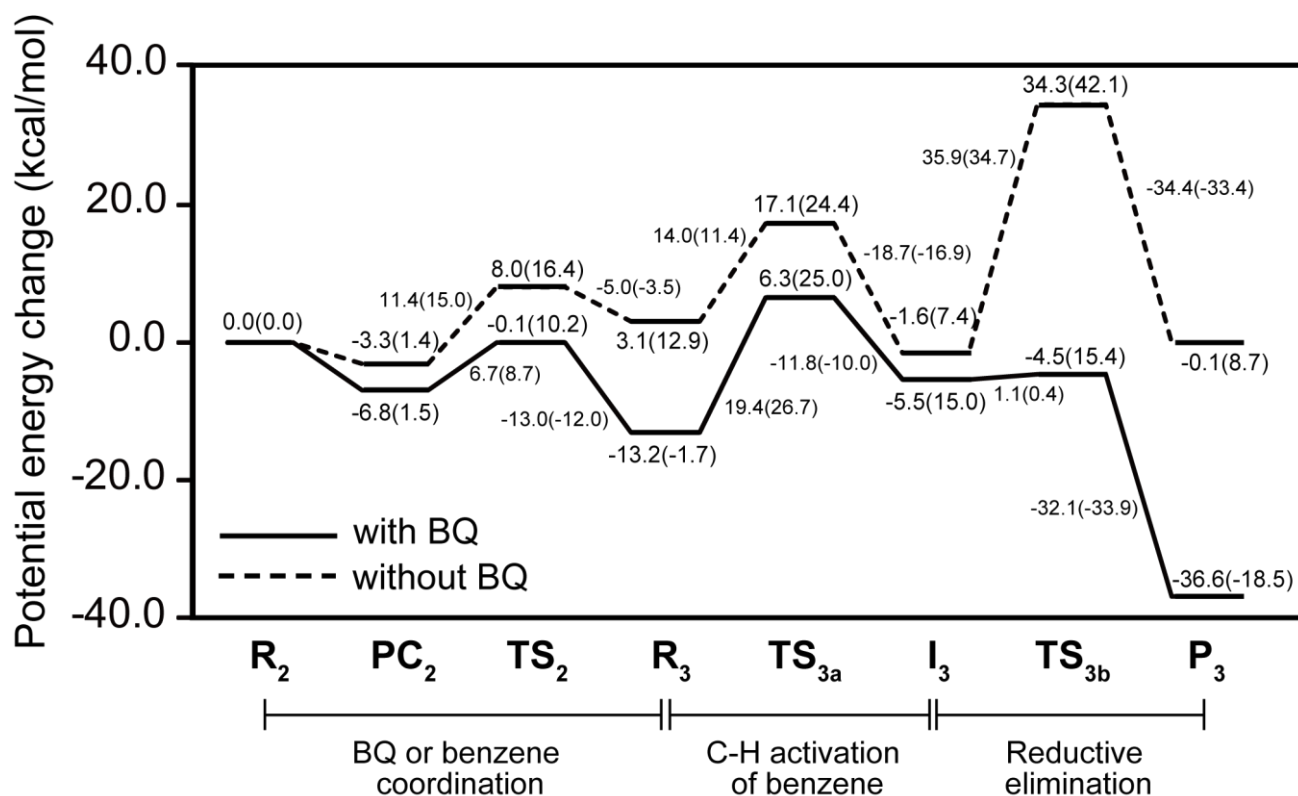
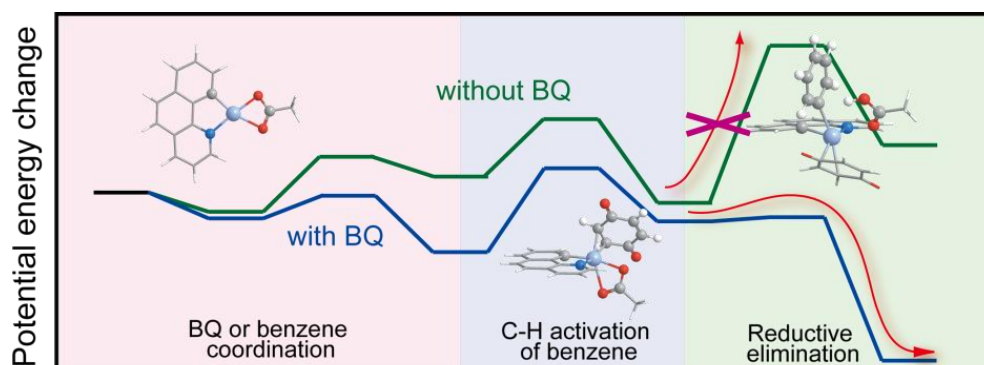


Fig. 11. Potential energy changes for the BQ or benzene coordination, the C-H activation of benzene, and the reductive elimination of Bzq-Ph, in the presence and absence of BQ in benzene. Energies^{a)} are given in kcal/mol unit. ^{a)} In parentheses are Gibbs free energy changes.

Graphical and Text Abstract



The direct cross-coupling reaction of benzene and benzo[*h*]quinoline (HBzq) catalyzed by Pd(OAc)₂ in the presence of benzoquinone (BQ) is theoretically investigated. Our study elucidated that BQ accelerates the reductive elimination (RE) step because BQ stabilizes the transition state and the product complex of RE by the back-donation interaction.

Electronic Supplementary Information

Pd(II)-Catalyzed Direct Cross-Coupling Reaction of Arenes via Highly Regioselective Aromatic C-H Activation: A Theoretical Study

Atsushi Ishikawa,^a Yoshihide Nakao,^a Hirofumi Sato,^a and Shigeyoshi Sakaki^{*a,b}

^a*Department of Molecular Engineering, Graduate School of Engineering, Kyoto University, Nishikyo-ku, Kyoto 615-8510, Japan, and* ^b*Fukui Institute for Fundamental Chemistry, Kyoto University, Nishi-hiraki cho, Takano, Sakyo-ku, Kyoto 606-8301, Japan*
(E-mail: sakaki@moleng.kyoto-u.ac.jp)

Contents

Complete reference 70.

Scheme S1: Large and small models for ONIOM method.

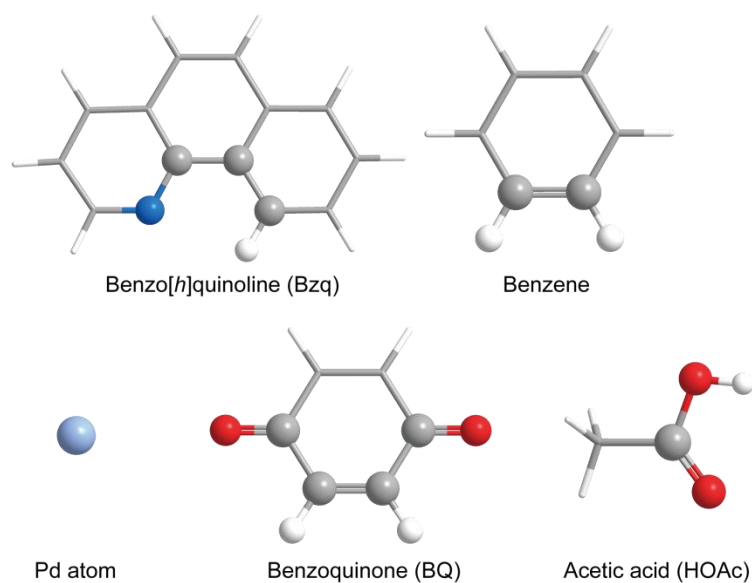
Fig. S1, S2, S3, and S4: Potential and Gibbs energy changes in gas phase.

Fig. S5: Potential and Gibbs energy changes of the C-H activation of benzene and the RE of Ph-Bzq, evaluated with DFT, MP2, MP4(SDQ) and ONIOM(CCSD(T):MP2) methods.

Table S1: Relative potential energies of the first C-H activation, BQ coordination, and the second C-H activation reactions calculated by Hartree-Fock, MP2, MP3, MP4(DQ), MP4(SDQ), and DFT(B3PW91) methods.

Complete Representation of Ref. 70

Frisch, M. J.; Trucks, G. W.; Schlegel, H. B.; Scuseria, G. E.; Robb, M. A.; Cheeseman, J. R.; Montgomery, J. A., Jr.; Vreven, T.; Kudin, K. N.; Burant, J. C.; Millam, J. M.; Iyengar, S. S.; Tomasi, J.; Barone, V.; Mennucci, B.; Cossi, M.; Scalmani, G.; Rega, N.; Petersson, G. A.; Nakatsuji, H.; Hada, M.; Ehara, M.; Toyota, K.; Fukuda, R.; Hasegawa, J.; Ishida, M.; Nakajima, T.; Honda, Y.; Kitao, O.; Nakai, H.; Klene, M.; Li, X.; Knox, J. E.; Hratchian, H. P.; Cross, J. B.; Bakken, V.; Adamo, C.; Jaramillo, J.; Gomperts, R.; Stratmann, R. E.; Yazyev, O.; Austin, A. J.; Cammi, R.; Pomelli, C.; Ochterski, J. W.; Ayala, P. Y.; Morokuma, K.; Voth, G. A.; Salvador, P.; Dannenberg, J. J.; Zakrzewski, V. G.; Dapprich, S.; Daniels, A. D.; Strain, M. C.; Farkas, O.; Malick, D. K.; Rabuck, A. D.; Raghavachari, K.; Foresman, J. B.; Ortiz, J. V.; Cui, Q.; Baboul, A. G.; Clifford, S.; Cioslowski, J.; Stefanov, B. B.; Liu, G.; Liashenko, A.; Piskorz, P.; Komaromi, I.; Martin, R. L.; Fox, D. J.; Keith, T.; Al-Laham, M. A.; Peng, C. Y.; Nanayakkara, A.; Challacombe, M.; Gill, P. M. W.; Johnson, B.; Chen, W.; Wong, M. W.; Gonzalez, C.; Pople, J. A. *Gaussian 03, Revision D.02*, Gaussian, Inc., Wallingford CT, 2004.



Scheme S1. Large model for ONIOM method. Atoms shown by balls are included in high level region which is calculated with the CCSD(T) while whole system is calculated by the lower level of theory.

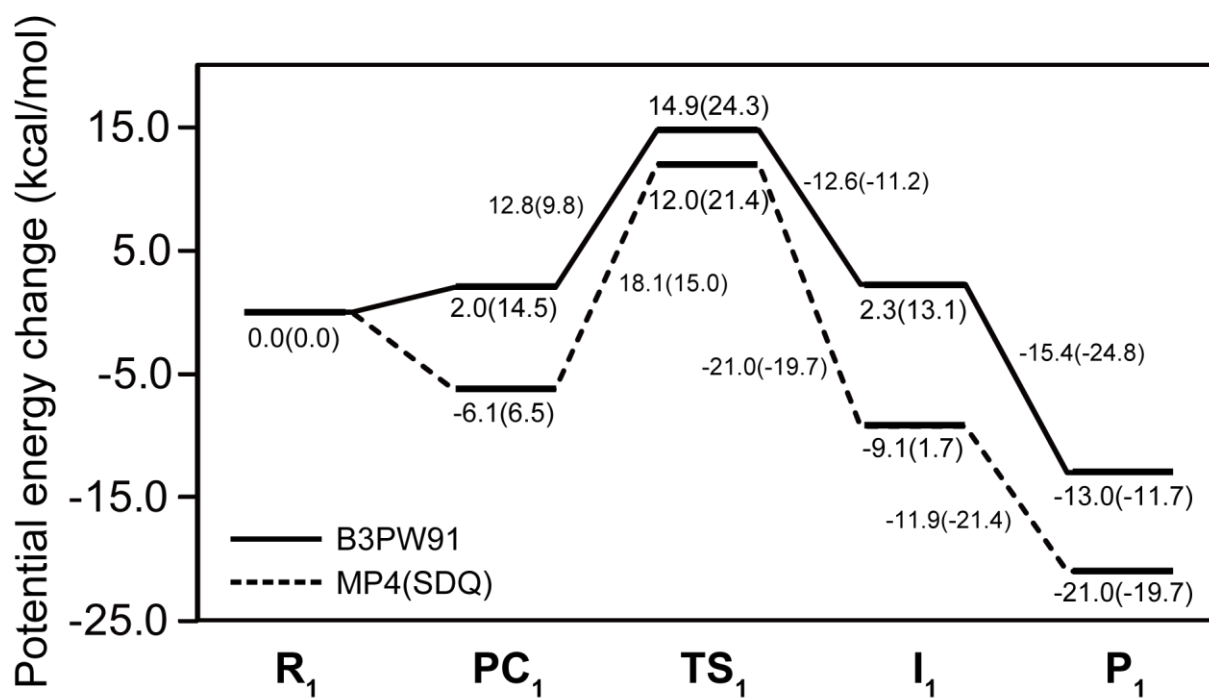


Fig. S1. Potential energy changes by the C-H activation of Bzq by $Pd(\eta^2-OAc)_2$ in gas phase. Energies^{a)} are given in kcal/mol unit. ^{a)} In parentheses are Gibbs free energy changes.

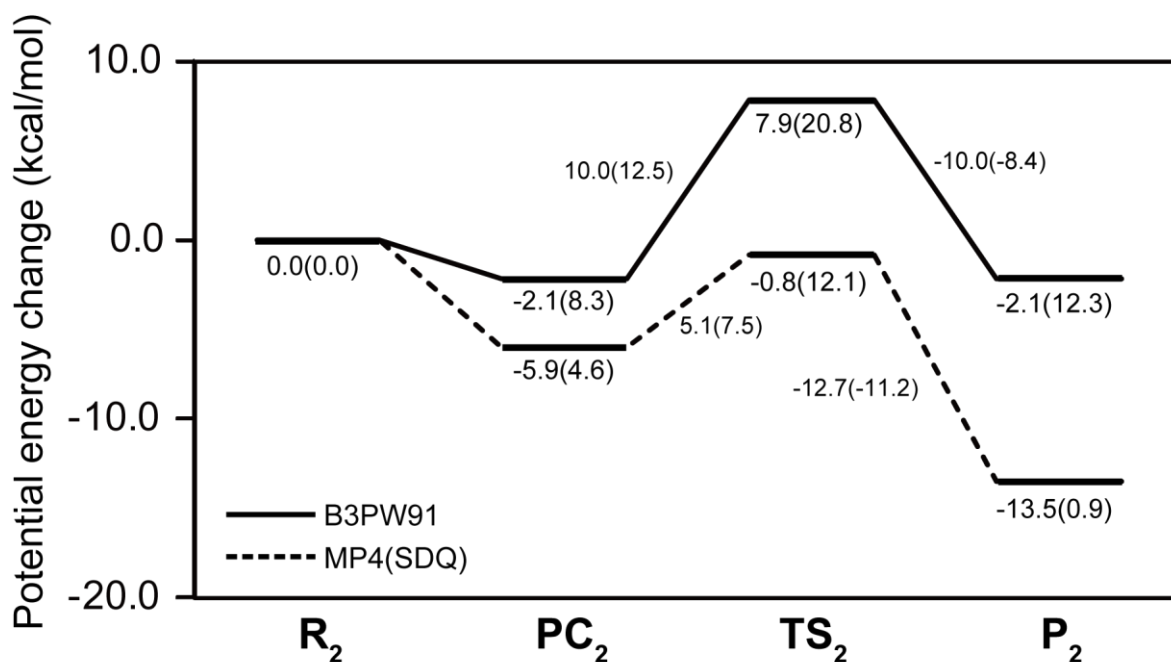


Fig. S2. Potential energy changes by BQ coordination to Pd(Bzq)(OAc) in gas phase. Energies^{a)} are given in kcal/mol unit. ^{a)} In parentheses are Gibbs free energy changes.

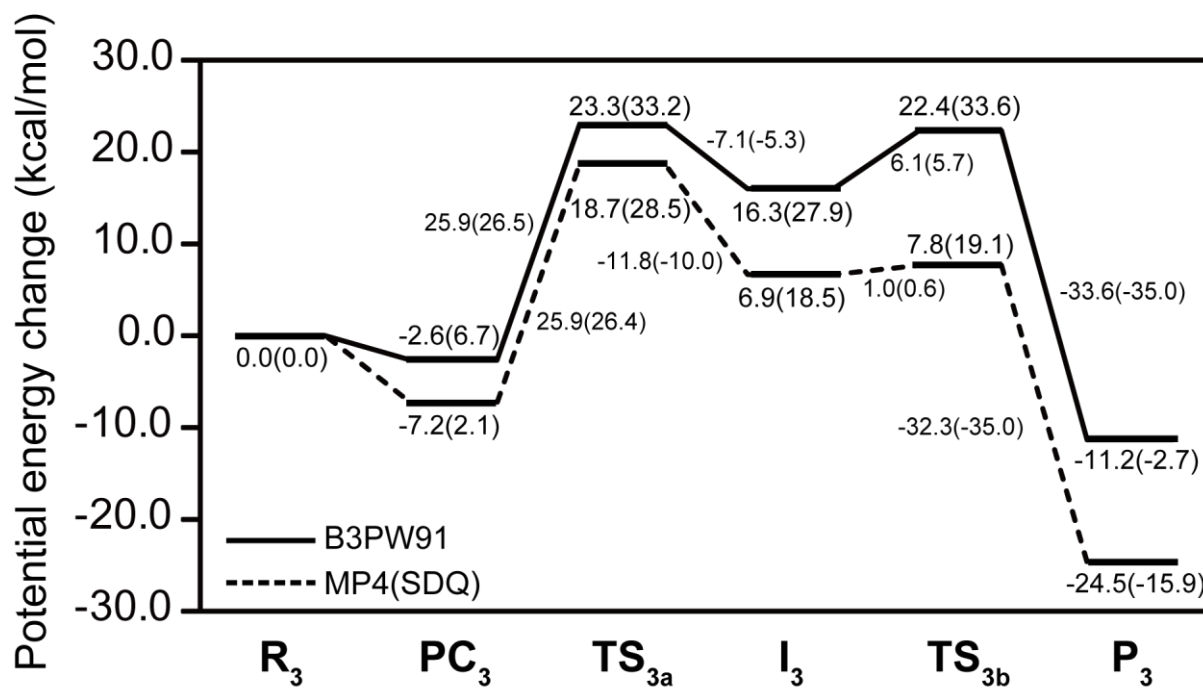


Fig. S3. Potential energy changes for the C-H activation of benzene by Pd(Bzq)(OAc)(BQ) in gas phase. Energies^{a)} are given in kcal/mol unit. ^{a)} In parentheses are Gibbs free energy changes.

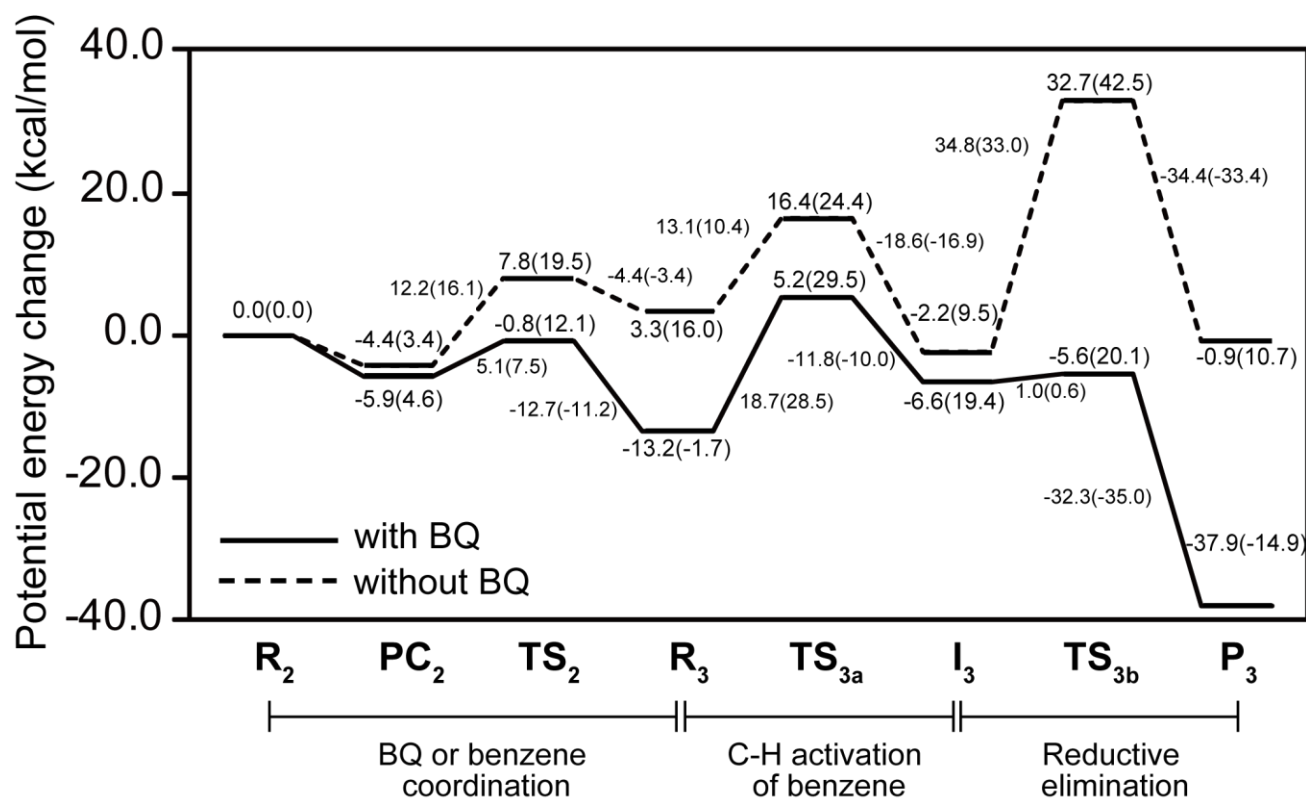


Fig. S4. Potential energy changes for the C-H activation of benzene by Pd(Bzq)(OAc)(BQ) in gas phase. Energies^{a)} are given in kcal/mol unit. ^{a)} In parentheses are Gibbs free energy changes.

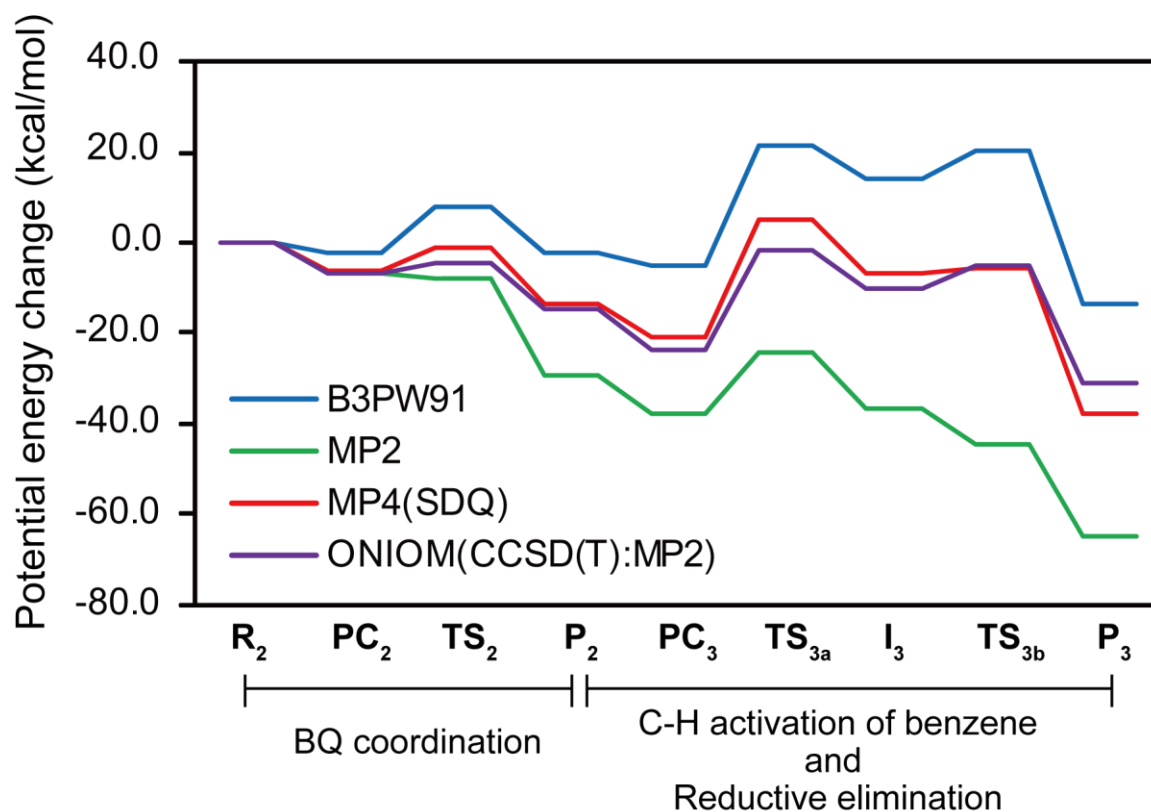


Fig. S5. Potential energy change of the BQ coordination, the C-H activation of benzene, and the reductive elimination in gas phase calculated with DFT, MP2, MP4(SDQ), and ONIOM(CCSD(T):MP2) methods. Energies are given in kcal/mol unit.

Table S1. Relative electronic energies of the C-H activation of HBzq, BQ coordination, and the C-H activation of benzene, calculated by Hartree-Fock, MP2, MP3, MP4(DQ), MP4(SDQ), and DFT(B3PW91) methods.^{a)} Energies are given in kcal/mol unit.

		HF	MP2	MP3	MP4(DQ)	MP4(SDQ)	B3PW91/BS-I	B3PW91
First C-H activation	R₁	0.0	0.0	0.0	0.0	0.0	0.0	0.0
	PC₁	12.7	-14.1	-2.5	-4.8	-6.1	-0.4	2.0
	TS_{1a}	35.2	1.6	14.2	13.4	12.0	14.5	14.9
	I₁	12.5	-19.8	-6.7	-9.7	-9.1	1.6	2.3
	P₁	-1.7	-32.8	-17.5	-21.9	-21.0	-13.3	-13.0
BQ coordination	R₂	0.0	0.0	0.0	0.0	0.0	0.0	0.0
	PC₂	-2.4	-7.0	-5.5	-5.5	-5.9	-4.0	-2.1
	TS₂	21.2	-7.7	4.0	2.0	-0.8	7.7	7.9
	P₂	25.7	-29.0	-1.0	-9.3	-13.5	-0.4	-2.1
	R₃	0.0	0.0	0.0	0.0	0.0	0.0	0.0
Second C-H activation and Reductive Elimination	PC₃	-3.4	-8.8	-7.0	-7.0	-7.2	-2.9	-2.6
	TS_{3a}	45.3	5.1	23.3	19.4	18.7	24.5	23.3
	I₃	30.0	-7.3	12.5	6.2	6.9	16.0	16.3
	TS_{3b}	43.4	-15.4	21.6	6.7	7.8	20.2	22.4
	P₃	-14.9	-35.6	-18.2	-27.3	-24.5	-16.8	-11.2

a) BS-II was used unless otherwise stated.